

## Dissociation of Pentameric to Monomeric C-Reactive Protein Localizes and Aggravates Inflammation

### In Vivo Proof of a Powerful Proinflammatory Mechanism and a New Anti-Inflammatory Strategy

Jan R. Thiele, MD\*; Jonathon Habersberger, MD\*; David Braig, MD; Yvonne Schmidt, MD; Kurt Goerendt; Valentin Maurer; Holger Bannasch, MD; Amelie Scheichl, MD; Kevin J. Woollard, PhD; Ernst von Dobschütz, MD; Frank Kolodgie, PhD; Renu Virmani, MD; G. Bjoern Stark, MD; Karlheinz Peter, MD, PhD†; Steffen U. Eisenhardt, MD†

**Background**—The relevance of the dissociation of circulating pentameric C-reactive protein (pCRP) to its monomeric subunits (mCRP) is poorly understood. We investigated the role of conformational C-reactive protein changes in vivo.

**Methods and Results**—We identified mCRP in inflamed human striated muscle, human atherosclerotic plaque, and infarcted myocardium (rat and human) and its colocalization with inflammatory cells, which suggests a general causal role of mCRP in inflammation. This was confirmed in rat intravital microscopy of lipopolysaccharide-induced cremasteric muscle inflammation. Intravenous pCRP administration significantly enhanced leukocyte rolling, adhesion, and transmigration via localized dissociation to mCRP in inflamed but not noninflamed cremaster muscle. This was confirmed in a rat model of myocardial infarction. Mechanistically, this process was dependent on exposure of lysophosphatidylcholine on activated cell membranes, which is generated after phospholipase A2 activation. These membrane changes could be visualized intravitaly on endothelial cells, as could the colocalized mCRP generation. Blocking of phospholipase A2 abrogated C-reactive protein dissociation and thereby blunted the proinflammatory effects of C-reactive protein. Identifying the dissociation process as a therapeutic target, we stabilized pCRP using 1,6-bis(phosphocholine)-hexane, which prevented dissociation in vitro and in vivo and consequently inhibited the generation and proinflammatory activity of mCRP; notably, it also inhibited mCRP deposition and inflammation in rat myocardial infarction.

**Conclusions**—These results provide in vivo evidence for a novel mechanism that localizes and aggravates inflammation via phospholipase A2-dependent dissociation of circulating pCRP to mCRP. mCRP is proposed as a pathogenic factor in atherosclerosis and myocardial infarction. Most importantly, the inhibition of pCRP dissociation represents a promising, novel anti-inflammatory therapeutic strategy. (*Circulation*. 2014;130:35-50.)

**Key Words:** atherosclerosis ■ C-reactive protein ■ inflammation ■ microcirculation ■ myocardial infarction

C-reactive protein (CRP) belongs to the pentraxin family of protein and circulates as a pentamer of 5 identical, noncovalently linked subunits in plasma. Recently, a dissociation mechanism on activated platelets that leads to a conformational change from the circulating native, pentameric CRP (pCRP) to its monomeric subunits (mCRPs) has been identified.<sup>1</sup> This dissociation is mediated by bioactive lipids<sup>2</sup> found on activated or damaged cells or platelets<sup>1,3</sup> and leads to an alteration of the proinflammatory profile of the protein.<sup>4</sup>

#### Clinical Perspective on p 50

With respect to the inflammatory properties of the 2 isoforms, it has been shown that dissociation of pCRP to mCRP leads to increased activation, adhesion, and transmigration of monocytes, as well as formation of reactive oxygen species in vitro,<sup>1</sup> which represent major pathophysiological factors that contribute to tissue injury in inflammation.

Recent animal work has suggested that injection of human pCRP can increase myocardial infarct size in a rat myocardial

Received October 31, 2013; accepted April 18, 2014.

From the University of Freiburg Medical Center, Department of Plastic and Hand Surgery (J.R.T., D.B., Y.S., K.G., V.M., H.B., G.B.S., S.U.E.) and Section of Endocrine Surgery, Clinic of General, Visceral and Thoracic Surgery, Academic Teaching Hospital University of Hamburg (E.v.D.), Reinbeck, Germany; Baker IDI Heart and Diabetes Institute, Melbourne, Victoria, Australia (J.H., A.S., K.P.); Imperial College London, Department of Medicine, London, United Kingdom (K.J.W.); and CVPPath Institute, Gaithersburg, MD (F.K., R.V.).

\*Drs Thiele and Habersberger contributed equally as first authors.

†Drs Peter and Eisenhardt contributed equally as last authors.

The online-only Data Supplement is available with this article at <http://circ.ahajournals.org/lookup/suppl/doi:10.1161/CIRCULATIONAHA.113.007124/-/DC1>.

Correspondence to Steffen U. Eisenhardt, MD, University of Freiburg Medical Center, Department of Plastic and Hand Surgery, Hugstetter Strasse 55, 79106 Freiburg, Germany. E-mail [steffen.eisenhardt@uniklinik-freiburg.de](mailto:steffen.eisenhardt@uniklinik-freiburg.de)

© 2014 American Heart Association, Inc.

*Circulation* is available at <http://circ.ahajournals.org>

DOI: 10.1161/CIRCULATIONAHA.113.007124

infarction model, which can be reduced by a CRP-blocking reagent.<sup>5</sup> In a vascular injury model in transgenic mice, CRP led to increased neointima formation.<sup>6</sup> Animal models of myocardial infarction,<sup>5,7</sup> stroke,<sup>8</sup> and intestinal ischemia/reperfusion<sup>9</sup> have found that infusion of CRP increases tissue damage. To date, it remains unclear whether the recently described pCRP dissociation to mCRP is of relevance in vivo and how it potentially contributes to the aforementioned findings. Furthermore, our understanding of the pathophysiology of CRP dissociation is mainly based on in vitro findings, and overall, the mechanisms and mediators involved are poorly understood.

Phospholipase A2 (PLA2) enzymes modify the composition of cellular membranes by releasing fatty acids from the sn2 position of phospholipids, which leads to the formation of arachidonic acid and lysophospholipids.<sup>10</sup> Arachidonic acid is further processed into bioactive eicosanoids, including prostaglandins and leukotrienes. Lysophospholipids can be further modified to platelet-activating factor (PAF). All these molecules are potent regulators of inflammation.<sup>10,11</sup> Because binding of CRP is enhanced on lysophosphatidylcholine-enriched membranes, we hypothesized that there is a link between PLA2 activation and CRP dissociation.

Here, we investigated the role of conformational changes in CRP in vivo and aimed to elucidate the underlying mechanisms, including the role of PLA2-mediated membrane changes. Furthermore, we aimed to identify the CRP dissociation process as a therapeutic target.

## Methods

### Reagents

pCRP purified from human ascites (Merck, Darmstadt, Germany) was dialyzed against phosphate-buffered physiological saline solution with Ca<sup>2+</sup> and Mg<sup>2+</sup> (PBS-Ca-Mg; Biochrom, Berlin, Germany) before use with a Slide-A-Lyzer Dialysis Cassette (Pierce Biotechnology, Rockford, IL). For subsequent application, the final concentration of pCRP was determined (BCA, Sigma-Aldrich, St. Louis, MO).<sup>12,13</sup> mCRP (1 mg/mL in Na-PBS) was used in the soluble, citraconylated form and prepared as described previously.<sup>14</sup> In awareness of potential problems with bacterial contamination in CRP preparations,<sup>15</sup> all reagents were tested for lipopolysaccharide (LPS) contamination with a *Limulus* assay (Sigma-Aldrich) and found to be below the detection limit (0.125 U/mL or 0.01 ng/mL LPS). CRP purity and spontaneous mCRP formation were ruled out by Western blotting with 1/20th of normal levels of sodium dodecyl sulfate of pCRP and mCRP preparations to avoid confounding by contamination of other CRP isoforms.

All animal studies were approved by the institutional review board of the University of Freiburg Medical Center (Freiburg, Germany), and procedures were performed in accordance with institutional guidelines. Studies that involved human tissue samples were approved by the institutional review committee, and the subjects gave informed consent to the use of the tissue samples for this study.

### Statistical Analysis

Analysis of data were performed with GraphPad Prism version 5.0 software (GraphPad Software, San Diego, CA). For comparison of 2 groups, a 2-tailed *t* test was used. A *P* value <0.05 was considered statistically significant. All experiments were performed  $\geq 3$  times. Data are expressed as mean $\pm$ SEM. A 1-way ANOVA to compare the effects of different treatments was used if >2 groups were compared. In case of significance, the Tukey test was used for pairwise comparison. Only significant results for both ANOVA and Tukey test are

presented. For analysis of the aptamer-specific binding to mCRP but not pCRP, we used a 1-way ANOVA with repeated measures to compare the groups with different concentrations. To analyze treatment effects over time, we performed a 2-way repeated-measures (mixed model) ANOVA with the fixed factors of time and treatment and the corresponding interaction term. Additionally, the random factor *animal* was included in the model. In case of a nonsignificant interaction and significant treatment effect, pairwise Bonferroni adjusted comparisons were performed at each time point. Significant results for both 2-way repeated-measures (mixed model) ANOVA and Bonferroni post hoc tests are presented.

An expanded Methods section is available in the online-only Data Supplement.

## Results

### CRP Is Deposited in Inflamed Human Tissue as mCRP and Colocalizes With Monocytes/Macrophages

In the human muscle biopsy samples of ischemia/reperfusion injury, we detected mCRP but not pCRP in the postischemic tissue samples, which colocalized with CD68-positive monocytes (Figure 1A). The postischemic increases in mCRP expression and CD68-positive cells showed a similar tendency (Figure 1B).

To analyze the potential relevance of mCRP deposition in the pathogenesis of tissue damage in humans, infarcted myocardial tissue samples were obtained from autopsy specimens that originated from patients who had had a myocardial infarction 2 to 4 days before death. Sections taken from infarcted and noninfarcted tissue were stained with antibodies specific for mCRP and pCRP. There was extensive deposition of mCRP in infarcted regions, with very limited deposition in noninfarcted areas (Figure 1C). We identified a perivascular distribution of mCRP staining.

Inflamed atherosclerotic plaques obtained from human carotid endarterectomy samples were stained with pCRP-, mCRP-, and CD68-specific antibodies (Figure 1D). mCRP was detected in the necrotic core of atherosclerotic lesions and colocalized with macrophages.

### CRP Aggravates the Inflammatory Response via Interaction With the Complement System, but CRP Does Not Show Intrinsic Proinflammatory Properties

In an intravital microscopy model of microcirculation changes in the rat cremaster muscle, low-dose LPS superfusion caused a mild inflammatory response that resulted in increased leukocyte rolling and adhesion (Figure 2A and 2B), as well as endothelial membrane changes, detected by in vivo annexin V staining of endothelial cells (Figure 2E). pCRP infusion did not induce leukocyte rolling or adhesion in the resting muscle tissue. In inflamed muscle tissue after LPS superfusion, CRP aggravated the preexisting inflammatory response as measured by leukocyte rolling, adhesion (Figure 2A and 2B), and monocyte transmigration (Figure 2C and 2D). Similar effects were observed in isolated rat monocytes ex vivo (Figure 2F).

The proinflammatory, tissue-damaging effects of human CRP in vivo are dependent on complement.<sup>7</sup> To show that the observed effects were dependent on this CRP-complement interaction and to exclude confounding by endogenous rat

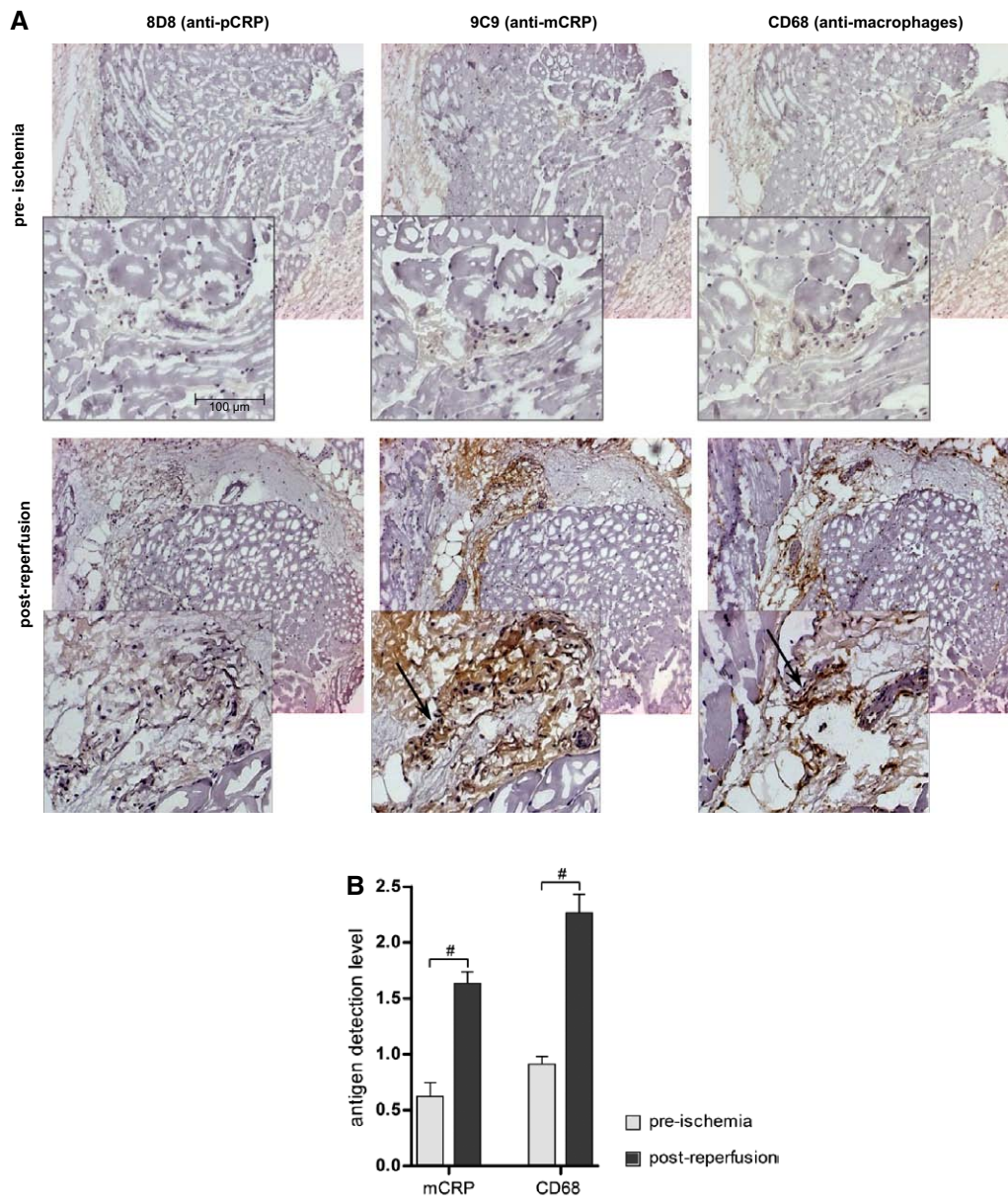


**Figure 1.** Accumulation of the monomeric subunit of C-reactive protein (mCRP) in inflamed human muscle tissue. **A**, Conformation-specific detection of C-reactive protein and CD68+ cells in striated human muscle tissue before (preischemia) and after (postreperfusion) free tissue transfer by immunohistochemistry. **Left**, Staining for pentameric C-reactive protein (pCRP); **middle**, staining for mCRP. Goat anti-mouse horseradish peroxidase-coupled antibody was used as secondary antibody. Typical results are shown. **B**, Quantification of immunohistochemical results. Given are relative values of immunoreactivity for mCRP and CD68. At least 3 nonoverlapping visual fields were evaluated and averaged from each sample. The average counted as the value for 1 sample. Values are mean $\pm$ SEM; n=11; # $P$ <0.05. The inflammatory response in ischemia/reperfusion led to a significant increase of mCRP deposition, which colocalized (arrows in **A**) with CD68+ leukocytes. **C**, Human postmortem samples after myocardial infarction demonstrated extensive deposition of mCRP in ischemic tissue. Although there was strong staining for mCRP in ischemic tissue, in noninfarcted areas there was only a small amount of mainly perivascular staining for mCRP. There was no significant staining of pCRP identified in any of the tissue segments or control samples. One example of 4 is shown. **D**, Detection of mCRP but not pCRP in human atherosclerotic plaques obtained by carotid endarterectomy. mCRP was localized to the necrotic core and colocalized with CD68+ cells. One example of 3 is shown. Positive staining is shown in green.

CRP, we analyzed the role of the complement system in CRP-induced leukocyte activation via depletion of complement. Intraperitoneal injection of cobra venom factor led to a significant reduction of complement activity compared with the control (Figure I in the online-only Data Supplement). Complement depletion induced a significant decrease in leukocyte rolling after 60 minutes and adhesion at 80 minutes in the CRP-driven inflammation (Figure I in the online-only Data Supplement).

These results indicate a dominant *in vivo* role of the complement system in the mCRP-triggered proinflammatory cascade.

#### CRP Is Transported Into Areas of Inflammation on Transmigrating Leukocytes and Is Deposited in Inflamed Tissue

Western blot analysis showed a deposition of CRP in LPS-challenged cremasteric muscle tissue but not in resting tissue

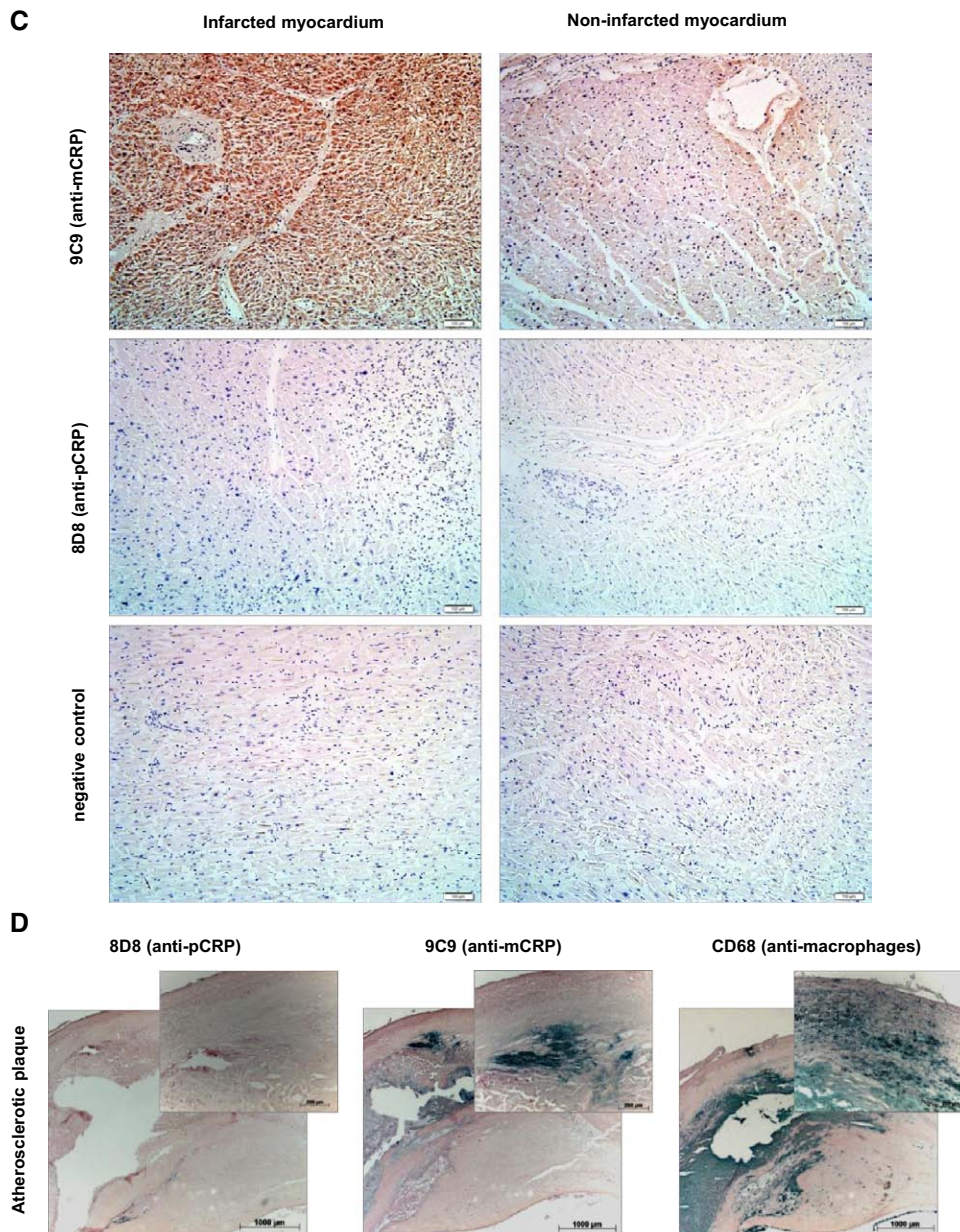


**Figure 1.** Continued

as evaluated for the triceps muscle and heart and lung tissue (Figure 3A through 3C). CRP in vivo tracking revealed that CRP could be detected on transmigrating leukocytes and was deposited in inflamed tissue (Figure 3D). Intravital staining of CRP and endothelial membrane changes (annexin V) showed that CRP/leukocyte transmigration was found in areas with endothelial membrane changes. In resting tissue, neither annexin V nor CRP was detected.

#### CRP Is Deposited as mCRP in Inflamed Tissue

Rat cremaster muscle samples were examined for CRP deposition by native Western blotting and immunohistochemistry by conformation-specific antibodies. Native Western blot analysis revealed that a majority of CRP deposited in the inflamed cremasteric tissue was in monomeric form. In non-inflamed tissue (without LPS superfusion), CRP was found

to a much reduced extent and only as pCRP (Figure 3E and 3F). This was verified by immunohistochemistry of rat cremasteric muscle after microcirculation experiments. In the control group and LPS group, no CRP was detected. After pCRP injection, without inflammatory stimulus to the cremasteric tissue, trace amounts of pCRP were detected by immunohistology. LPS-induced localized cremasteric inflammation led to deposition and detection of mCRP (Figure 3G and 3H).

#### mCRP Induces Adhesion of Human and Rat Monocytes and Generation of ROS

In an in vitro monocyte adhesion assay, mCRP induced a significant increase in leukocyte adhesion to a fibrinogen matrix compared with the control that was comparable to high-dose stimulation with LPS in both rat (Figure 4A) and human (Figure 4B) monocytes. This finding underlines the physiological

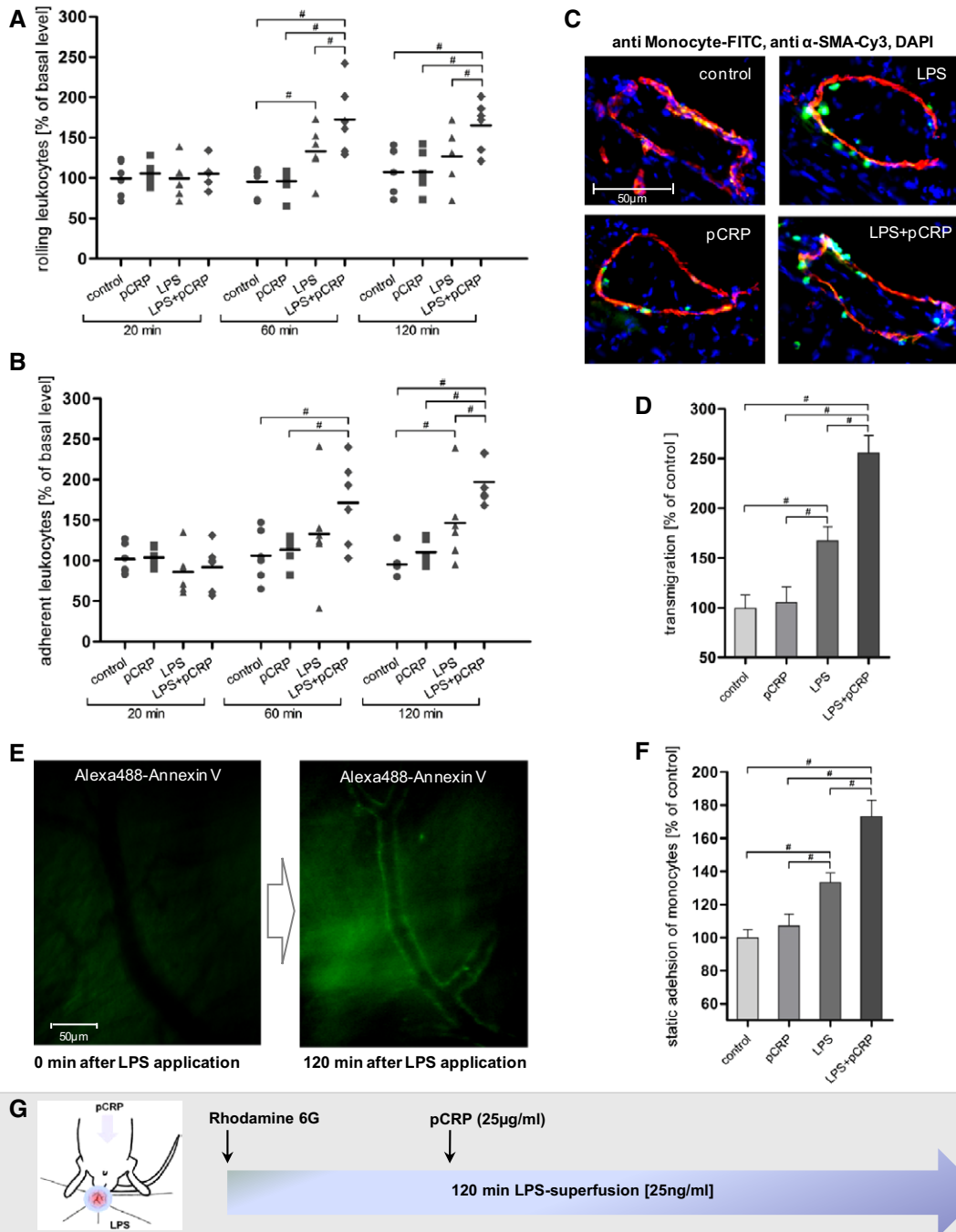


**Figure 2.** Pentameric C-reactive protein (pCRP) significantly increased leukocyte rolling after 60 minutes (A) and adhesion at 120 minutes (B) in lipopolysaccharide (LPS)-induced inflammation in rat cremasteric postcapillary venules. Leukocyte-endothelium interaction was analyzed by intravital microscopy under superfusion with LPS (25 ng/mL) with or without intravenous injection of pCRP (25  $\mu$ g/mL). Leukocytes were labeled with rhodamine 6G. Count at 0 minutes was set to 100%. Dot plots and mean of 6 rats are shown; # $P$ <0.05. C, Immunofluorescence detection of monocyte/macrophage transmigration in the inflamed cremasteric tissue with fluorescein isothiocyanate (FITC)-anti-rat monocyte antibody. The vessel wall was stained by a Cy3-anti  $\alpha$ -smooth muscle actin (SMA) antibody. Representative results are shown.  $n=6$  rats per group. D, Quantification of immunofluorescence results. Three slides of each animal were analyzed and averaged. The average counted as the value for 1 rat ( $n=6$  rats per group). Mean cell count of the control was set to 100%; # $P$ <0.05. Values are mean $\pm$ SEM. pCRP application significantly increased transmigration in the LPS-stimulated tissue. E, In vivo phosphatidylserine expression in LPS-stimulated cremasteric tissue. Phosphatidylserine expression was detected by intravenous application of Alexa Fluor 488-annexin V (500  $\mu$ L/kg body weight) 20 minutes before addition of LPS. Representative results are shown ( $n=3$  rats). Endothelium-associated phosphatidylserine expression is strongly induced by LPS. F, Static rat monocyte adhesion assay after stimulation with LPS (25 ng/mL) with or without pCRP (25  $\mu$ g/mL). Adherent cells were quantified in a phosphatase-substrate reaction. Values are mean $\pm$ SEM. Experiments were performed in triplicate ( $n=3$  rats). Representative results are shown. Addition of pCRP significantly increased monocyte adhesion under LPS. pCRP alone had no effect. G, Flow chart of the intravital experimental protocol.

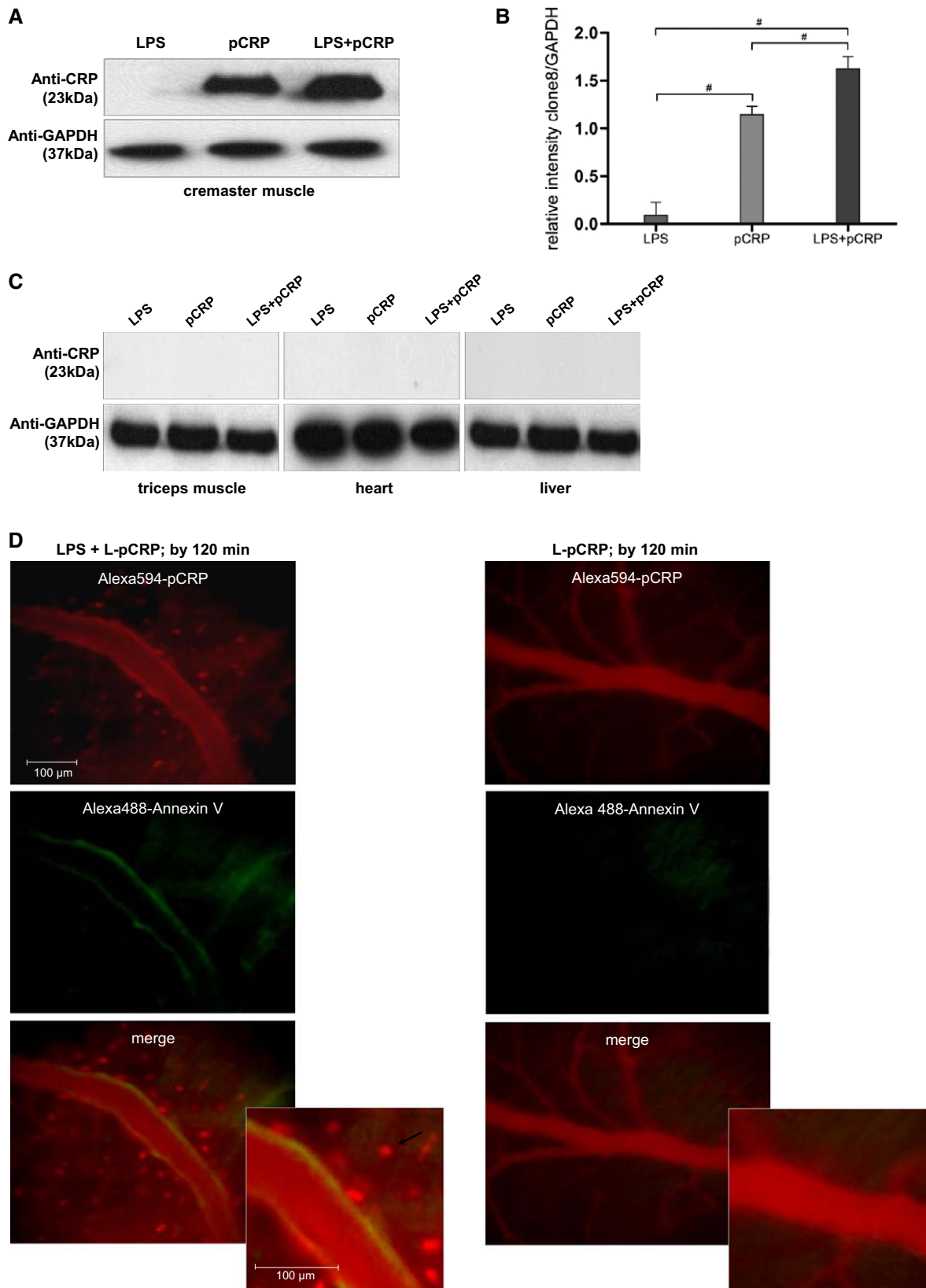


**Figure 3.** Pentameric C-reactive protein (pCRP) accumulates in inflammation and binds to transminating leukocytes. **A–C**, Western blot analysis of rat tissue after cremasteric superfusion with lipopolysaccharide (LPS; 25 ng/mL) with or without intravenous application of pCRP (25 μg/mL) by 20 minutes. Anti-CRP antibody clone 8 was applied. GAPDH served as loading control. A typical result of cremasteric tissue from 3 different animals is shown (**A**), and quantification is illustrated (**B**). Relative values are given for immunoreactivity for clone 8 related to the signal of GAPDH. Values are mean±SEM; #P<0.05. Deposition of C-reactive protein (CRP) in the cremasteric tissue was increased significantly through LPS-induced inflammation. **C**, Triceps muscle, heart, and liver did not accumulate CRP. (**Continued**)

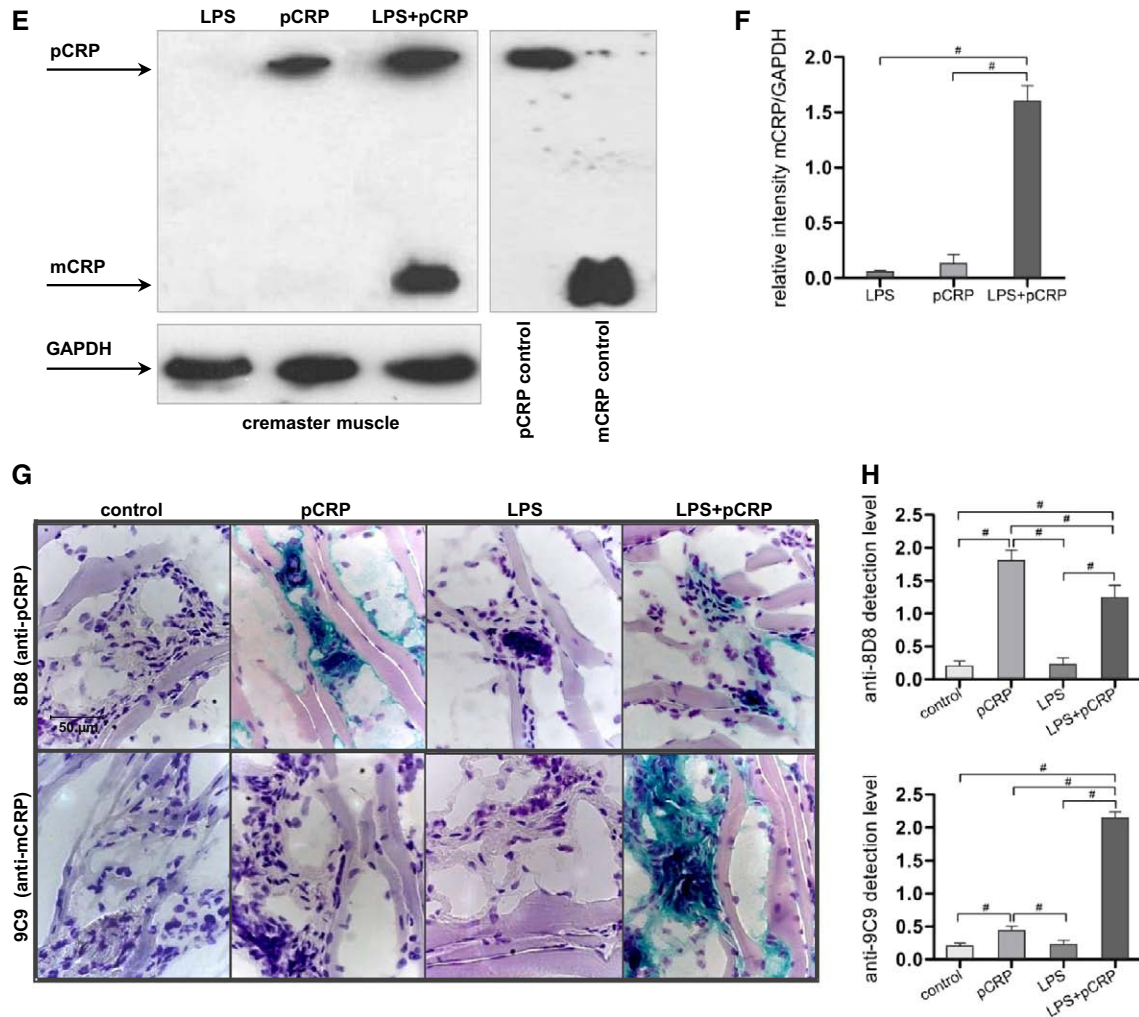


**Figure 3. Continued D,** CRP in vivo tracking by intravital microscopy. Before intravenous injection, pCRP (25  $\mu\text{g}/\text{mL}$ ) was fluorescently labeled with Alexa Fluor 594 (L-pCRP). Local inflammation was achieved by cremasteric superfusion with LPS (25  $\text{ng}/\text{mL}$ ; left lane). Endothelial activation/impairment was confirmed via Alexa Fluor 488–annexin V (500  $\mu\text{L}/\text{kg}$  body weight) positive phosphatidylserine expression. In the inflamed (left lane) but not in the resting (right lane), cremasteric tissue, pCRP bound to activated leukocytes (arrow) and, with them, extravasated into the perivascular tissue. Representative images are shown;  $n=3$  per group. **E,** Dissociation of pCRP to monomeric subunit of C-reactive protein (mCRP) in acute inflammation. Western blot of native PAGE (1/20th SDS) of rat cremasteric tissue after treatment with LPS (25  $\text{ng}/\text{mL}$ ) for 120 minutes with or without intravenous application of pCRP after 20 minutes. Both pCRP and mCRP were detected with the anti-CRP antibody clone 8. pCRP solution and predissociated mCRP solution served as controls. A typical result from 3 experiments is shown. **F,** Quantification of Western blot results. Relative values of immunoreactivity for mCRP normalized to signal intensity of anti-GAPDH staining are shown. Values are mean  $\pm$  SEM;  $\#P<0.05$ . In inflamed cremasteric tissue, accumulated pCRP was in large part dissociated to mCRP. mCRP was not detectable in resting tissue. **G,** Immunohistochemical staining of the cremaster muscle with HistoGreen after superfusion with LPS (25  $\text{ng}/\text{mL}$ ) with or without intravenous application of pCRP (25  $\mu\text{g}/\text{mL}$ ). Clone 8D8 was used to detect pCRP and clone 9C9 to detect mCRP. Representative results are shown ( $n=6$  per group). **H,** Quantification of immunohistochemical results. Relative values of immunoreactivity for pCRP and mCRP are shown. Three nonoverlapping visual fields were evaluated and averaged for each rat. The average counted as value for 1 rat ( $n=6$ );  $\#P<0.05$ . pCRP was detected in the cremasteric tissue 120 minutes after intravenous application with or without treatment with LPS, although positive staining was more pronounced in the resting muscle tissue. LPS-triggered inflammation led to a significant increase of interstitial mCRP deposition.

relevance of data obtained in the rat model to human disease processes. mCRP induced ROS generation as a major component of inflammatory tissue damage (Figure 4F). Furthermore, these results indicate that mCRP was the proinflammatory isoform of CRP responsible for producing the inflammatory effects.

### mCRP Is Responsible for the Proinflammatory Activity of CRP

Predissociated mCRP induced leukocyte rolling (after 30 minutes) and adhesion (at 60 minutes) in cremasteric muscle

venules (Figure 4C and 4D). Without existing inflammatory tissue damage, pCRP injection did not show effects on leukocyte rolling and adhesion.

### Proinflammatory mCRP Effects on Monocytes Are Mediated by Fc $\gamma$ -RI and III Signaling

Fc $\gamma$  receptors have been implicated in the signaling of mCRP effects.<sup>1</sup> To establish the specific role of these receptors, small interfering RNA knockdowns of the 3 major Fc $\gamma$  receptors, Fc $\gamma$ -RI (CD64), Fc $\gamma$ -IIa (CD32), and Fc $\gamma$ -III (CD16),

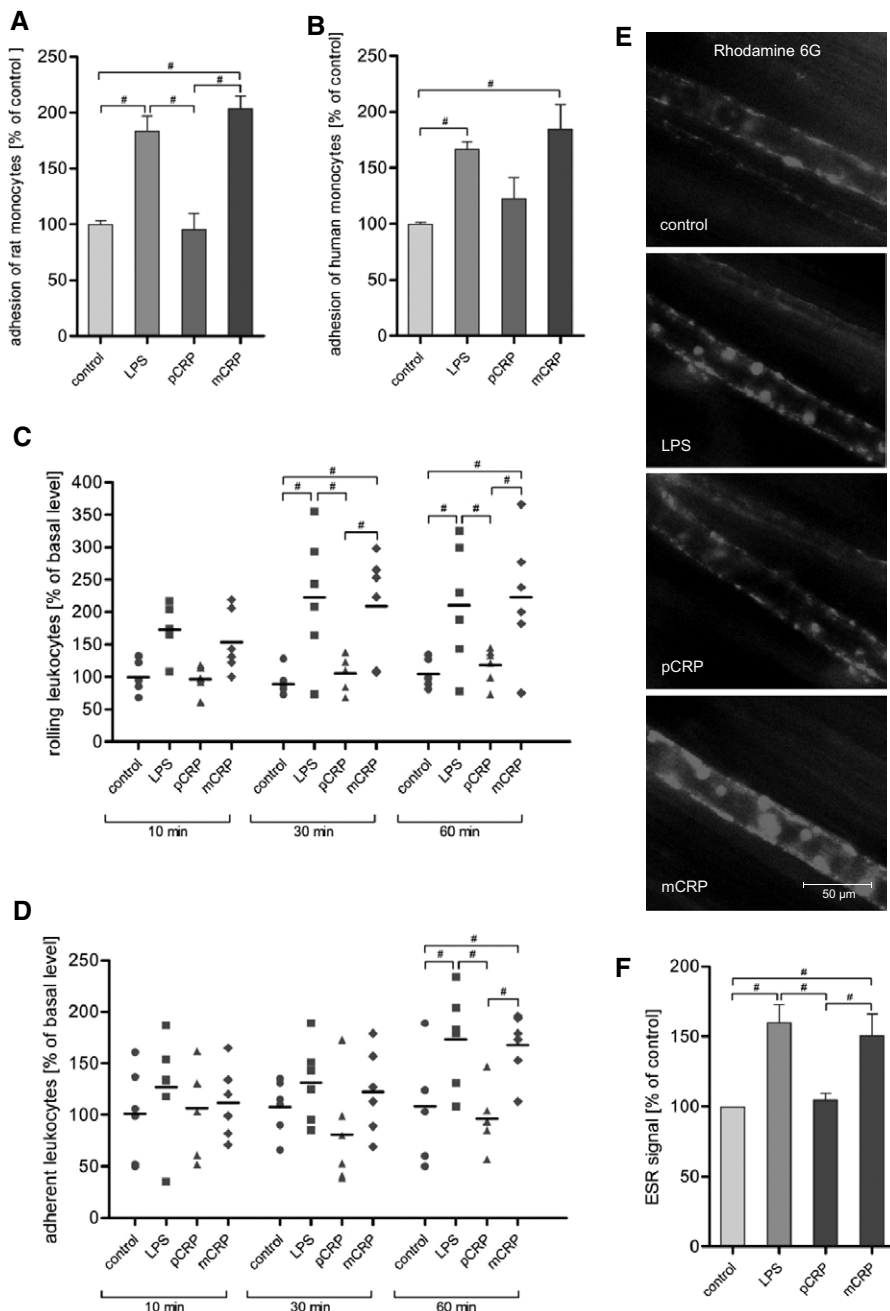


**Figure 4.** Proinflammatory effects of ex vivo predissociated monomeric subunit of C-reactive protein (mCRP) in vitro and in vivo. Static adhesion assay of rat (**A**) and human (**B**) monocytes that were incubated with either pentameric C-reactive protein (pCRP) or mCRP at 25 µg/mL for 60 minutes. Adherent cells were quantified. PBS control was set to 100%. Lipopolysaccharide (LPS) 50 µg/mL served as positive control. Mean±SEM values are given. Experiments were performed in triplicate; n=3; #P<0.05. Representative results are shown. mCRP induced a significant increase in monocyte adhesion. **C–E**, In vivo leukocyte-endothelium interaction under intravenous injection of either mCRP or pCRP (25 µg/mL) analyzed by intravital microscopy. Superfusion of the cremaster muscle with LPS (1 µg/mL) served as positive control. Counts at 0 minutes were set to 100%. Dot plots and mean of 6 rats are shown; #P<0.05. mCRP significantly increased leukocyte rolling after 30 minutes (**C**) and leukocyte adhesion at 60 minutes (**D**), whereas pCRP showed no significant effect compared with the control. **E**, Typical examples for venules of the 4 groups after 30 minutes. **F**, Reactive oxygen species formation in rat monocytes after in vivo exposure to pCRP and mCRP. After intravital microscopy, electron spin resonance spectroscopy (ESR) was performed in isolated monocytes with CMH (25 µg/mL) as a spin label. Values are mean±SEM of 4 different rats; #P<0.05. Reactive oxygen species formation in rat monocytes was significantly induced by mCRP in vivo.

were performed on harvested donor monocytes. Reverse-transcription polymerase chain reaction revealed successful knockdown of the 3 receptors in the target groups compared with the control groups that were transfected with scrambled small interfering RNA sequences (Figure IIA in the online-only Data Supplement). The reduction in surface expression of the respective receptors was confirmed by flow cytometry (Figure IIB in the online-only Data Supplement). Knockdown of Fcγ-RI and Fcγ-III significantly reduced mCRP binding to monocytes compared with the corresponding scrambled control as determined by confocal microscopy, exemplarily shown for Fcγ-III in Figure IIF in the online-only Data Supplement. The addition of mCRP led to receptor clustering and colocalization with mCRP in native monocytes. In

static monocyte adhesion assays, proinflammatory mCRP effects were significantly reduced in the Fcγ-RI knockdown (Figure IIC in the online-only Data Supplement) and Fcγ-RIIIa knockdown group compared with the corresponding mCRP control group (Figure IIE in the online-only Data Supplement). Knockdown of Fcγ-RIIa did not have a significant effect on mCRP-mediated monocyte adhesion (Figure IID in the online-only Data Supplement).

#### Inhibition of PLA2 Prevents CRP Dissociation on Activated Cells

Several inhibitors of enzymes of the PLA2 family were used to analyze the effects on CRP dissociation. By native gel Western blot analysis, we were able to detect CRP dissociation on



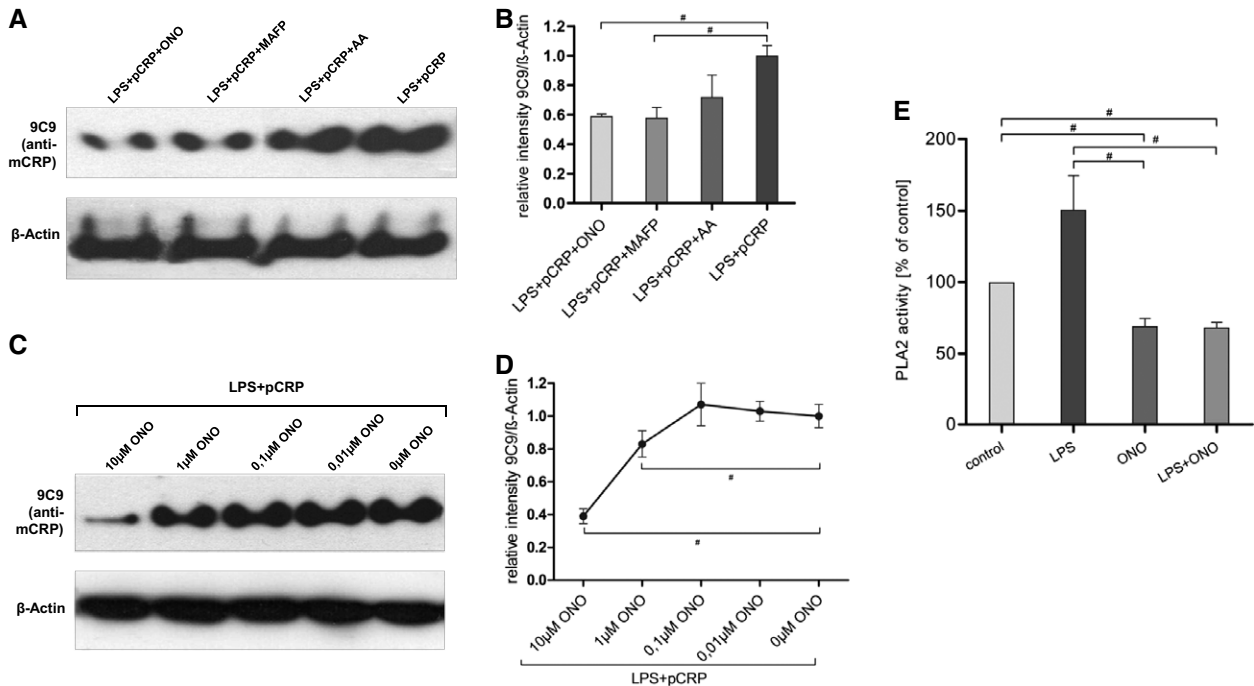


**Figure 5.** Prevention of formation of monomeric subunit of C-reactive protein (mCRP) by inhibition of phospholipase A2 (PLA2). **A**, Western blot of native PAGE with 1/20th SDS of human monocytes stained for mCRP with clone 9C9 after incubation with the PLA2 inhibitors ONO-RS-082 (ONO; 20  $\mu$ mol/L), methyl arachidonyl fluorophosphonate (MAFP; 20  $\mu$ mol/L), and aristolochic acid (AA; 10  $\mu$ mol/L) for 20 minutes followed by incubation with pentameric C-reactive protein (pCRP; 25  $\mu$ g/mL) with or without lipopolysaccharide (LPS; 25 ng/mL) for another 60 minutes.  $\beta$ -Actin served as loading control. A typical result of 3 experiments is shown. **B**, Quantification of Western blot results. Relative values of immunoreactivity for mCRP normalized to  $\beta$ -actin signal are shown. Values are mean $\pm$ SEM; # $P$ <0.05. Inhibition of PLA2 by ONO and MAFP of activated human monocytes significantly reduced mCRP formation. **C**, Western blot of native PAGE with 1/20th SDS of human monocytes stained for mCRP with clone 9C9 after incubation with ONO at concentrations from 10 to 0.01  $\mu$ mol/L for 20 minutes followed by incubation with pCRP (25  $\mu$ g/mL) plus LPS (25 ng/mL) for another 60 minutes. A typical result of 3 experiments is shown. **D**, Quantification of Western blot results. Given are relative values of immunoreactivity for mCRP normalized to  $\beta$ -actin signal. Values are mean $\pm$ SEM; # $P$ <0.05. ONO inhibited mCRP formation in a concentration-dependent manner. **E**, Quantification of PLA2 activity in mononuclear leukocytes after treatment with LPS 25 ng/mL with or without ONO 20  $\mu$ mol/L. Induction of PLA2 activity by exposition to LPS was decreased significantly by addition of ONO as measured by cleavage of a PLA2-specific fluorescent substrate. Mean $\pm$ SEM values are given. Experiments were performed in triplicate;  $n$ =3; # $P$ <0.05. Representative results are shown.

activated monocytes, as described previously.<sup>1</sup> Inhibition of PLA2 by ONO-RS, methyl arachidonyl fluorophosphonate, and aristolochic acid reduced mCRP formation, which suggests that CRP dissociation was mediated by expression of lysophosphatidylcholine (LPC) on cells through activation of PLA2 (Figure 5A and 5B).

In vitro experiments demonstrated that LPS-induced PLA2 activity in mononuclear leukocytes could be decreased by pre-incubation of cells with ONO-RS (Figure 5E), thereby inhibiting the mCRP formation in a concentration-dependent manner, as evaluated by native gel electrophoresis. Concentrations of 10  $\mu$ mol/L ONO-RS were able to produce a near-complete inhibition of CRP dissociation (Figure 5C and 5D).

### Inhibition of PLA2 In Vivo Inhibits Localized mCRP Formation and Leukocyte Activation

Using a concentration of 10  $\mu$ mol/L ONO-RS superfusion of the cremasteric muscle tissue, we were able to demonstrate complete inhibition of the effects of CRP on leukocyte rolling at 120 minutes and on adhesion after 60 minutes. In contrast, LPS-mediated proinflammatory effects were not significantly inhibited compared with the LPS control (Figure 6A and 6B). This demonstrates that blocking of PLA2 in vivo inhibits mCRP generation and thereby prevents amplification of the inflammatory response. Localized CRP dissociation was observed intravitaly by tracking

of fluorescently labeled pCRP and detection of mCRP by an mCRP-specific fluorescently labeled aptamer.<sup>16</sup> Control experiments demonstrated that the aptamer was specific for mCRP and did not possess potential proinflammatory confounding effects (Figure 6D and 6E). In vivo mCRP generation and transmigration into inflamed tissue were observed. This was abolished by blocking PLA2 with ONO-RS (Figure 6C). Because of the inhibition of mCRP generation, the fluorescently labeled pCRP remained detectable. This was associated with a lack of CRP detection in the inflamed tissue.

### Stabilization of CRP and Prevention of CRP Dissociation Inhibits Proinflammatory CRP Properties In Vivo

1,6-Bis(phosphocholine)-hexane (1,6-bis PC) is able to stabilize pCRP in a decameric conformation and is able to inhibit its interactions with complement.<sup>5</sup> We demonstrated here that 1,6-bis PC also inhibited CRP dissociation to mCRP (Figure 7A and 7B) in vitro. Using this stabilization of pCRP before injection, we demonstrated by native Western blotting of inflamed cremasteric tissue that 1,6-bis PC inhibited CRP deposition in inflamed tissue (Figure 7C). These data were confirmed by immunohistochemistry, which demonstrated that mCRP deposition in the inflamed muscle tissue was markedly decreased

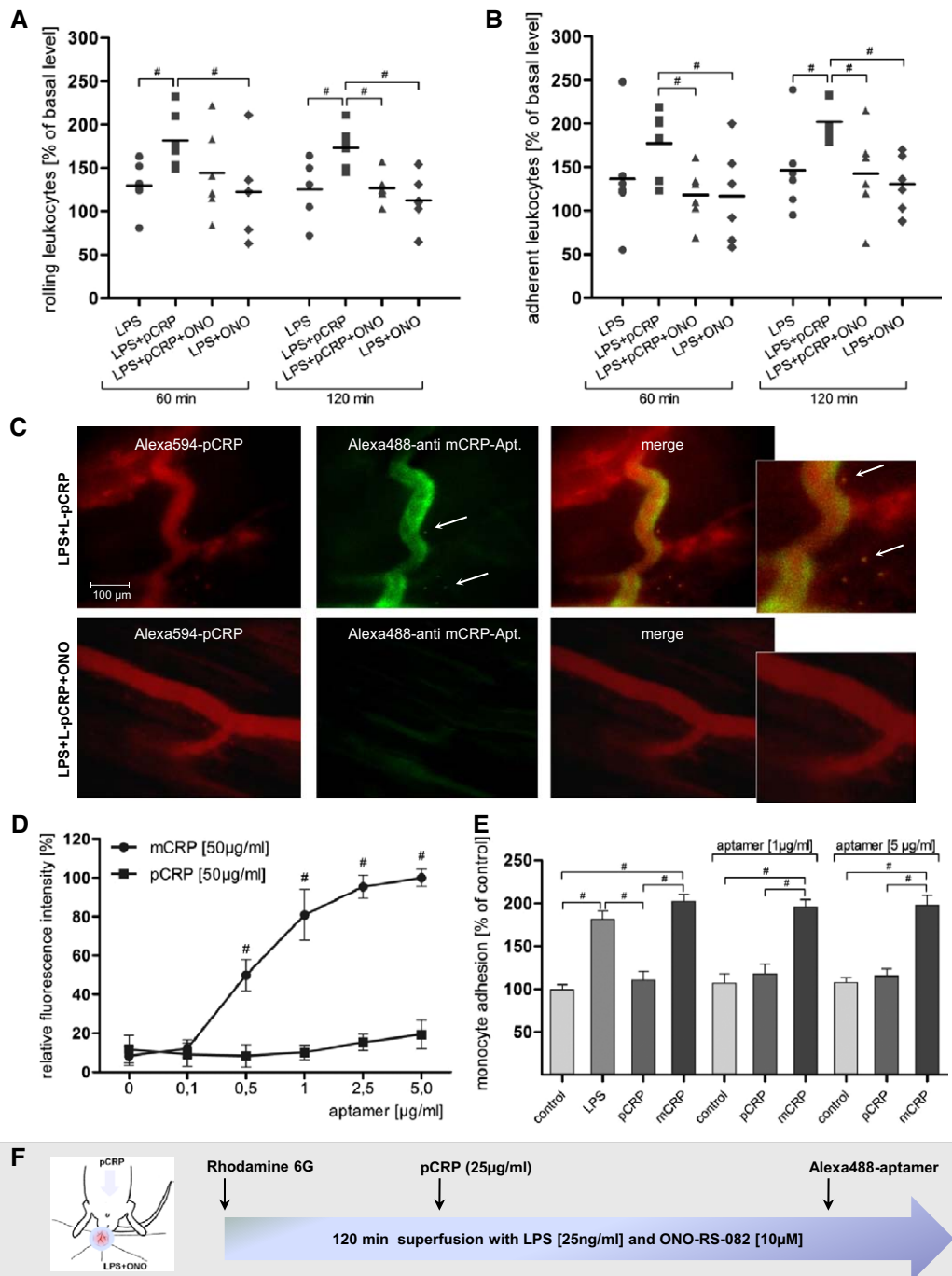


**Figure 6.** Prevention of C-reactive protein (CRP)–mediated inflammation by inhibition of phospholipase A2 (PLA2). Evaluation of leukocyte rolling (**A**) and adhesion (**B**) by intravital microscopy after cremasteric superfusion with lipopolysaccharide (LPS; 25 ng/mL) and ONO-RS-082 (ONO; 10 μmol/L) with or without intravenous application of pentameric CRP (pCRP; 25 μg/mL). Dot plots and mean of 6 rats are shown;  $\#P < 0.05$ . ONO prevented the CRP-induced proinflammatory potential on circulating leukocytes in LPS-triggered inflammation, with a significant decrease of leukocyte rolling (**A**) at 120 minutes and a significant reduction of leukocyte adhesion (**B**) after 60 minutes. **C**, Conformation-specific immunofluorescence detection of pCRP and monomeric subunit of C-reactive protein (mCRP) in vivo. pCRP was fluorescently labeled with Alexa Fluor 594 (L-pCRP). In vivo detection of mCRP was conducted by intravenous injection of mCRP binding Alexa Fluor 488–labeled aptamer (mCRP-Apt; 2.5 μg/mL) after 100 minutes and subsequent intravital imaging after 120 minutes. mCRP was detected in vivo in inflamed tissue by mCRP-specific aptamer binding. In LPS-triggered inflammation, mCRP was detected intravascularly and on transmigrating leukocytes (arrows). Cremasteric superfusion with ONO abrogated the formation of mCRP in acute inflammation. Representative results are shown;  $n = 3$ . **D**, In vitro binding of mCRP-Apt to pCRP and mCRP quantified by fluorescence spectroscopy. Mean  $\pm$  SEM values are given.  $\#P < 0.05$  compared with the corresponding value under pCRP. mCRP could be detected specifically by the aptamer, with a significant increase in fluorescence signal at concentrations of 0.5 μg/mL compared with the pCRP group. **E**, Proinflammatory testing of mCRP-Apt in a static monocyte adhesion assay in the presence or absence of CRP isoforms after 60 minutes of treatment. Experiments were performed in triplicate; PBS control was set to 100%. Values are mean  $\pm$  SEM;  $\#P < 0.05$ . mCRP-Apt had no intrinsic proinflammatory potential and showed no significant impact on the proinflammatory potential of mCRP. **F**, Flow chart of the intravital experimental protocol.

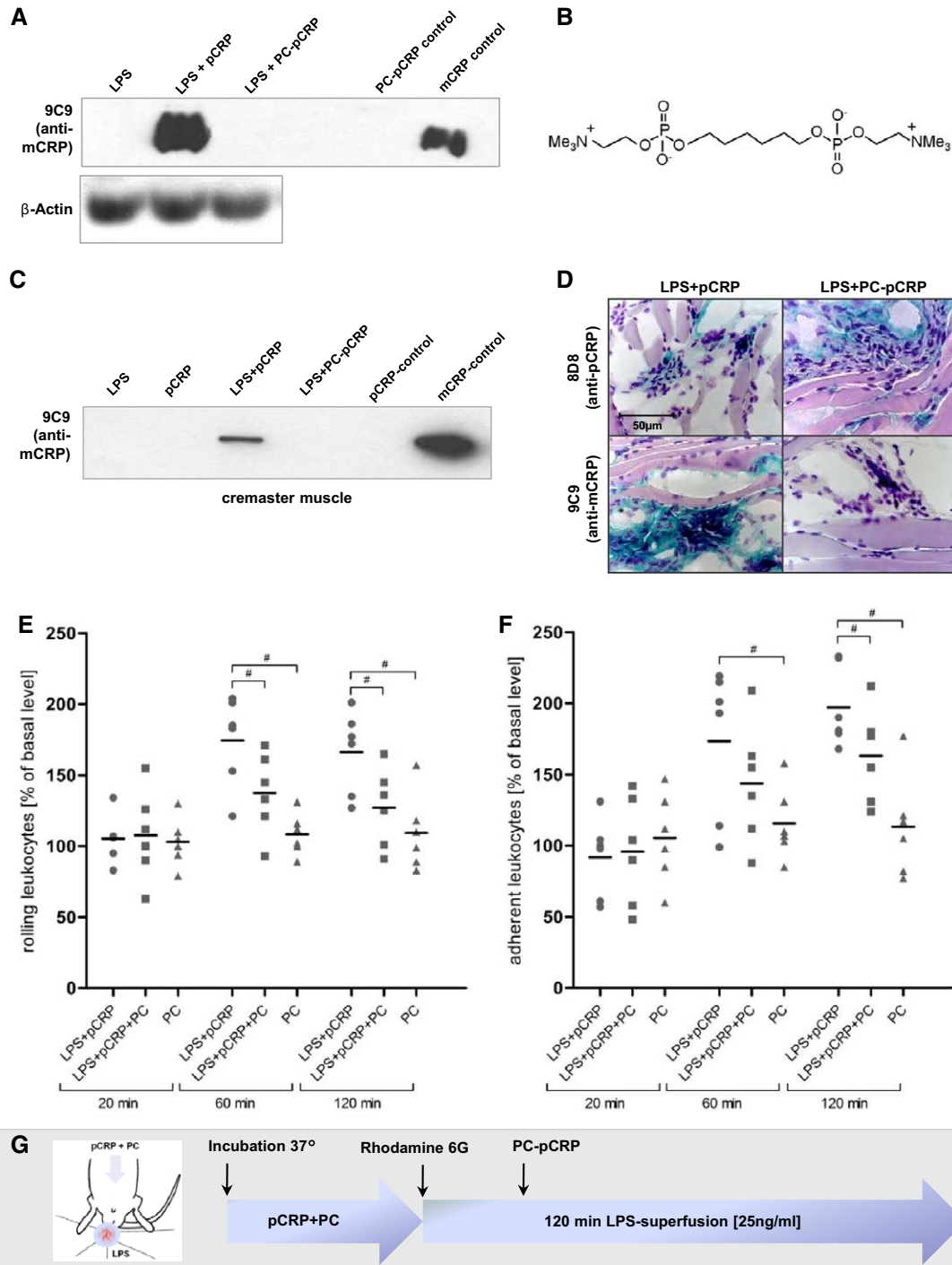


**Figure 7.** Prevention of pentameric C-reactive protein (pCRP) dissociation by decameric stabilization. **A**, Western blot of native PAGE (1/20th SDS) of human monocytes stained for monomeric subunit of C-reactive protein (mCRP) after stabilization of pCRP with 1,6-bis(phosphocholine) (PC), which was administered for 60 minutes after preincubation with lipopolysaccharide (LPS; 25 ng/mL; 20 minutes). A typical result from 3 experiments is shown. PC prevented dissociation of pCRP to mCRP on activated monocytes. **B**, Chemical structure of PC. **C**, Detection of mCRP in LPS-inflamed cremasteric tissue after intravenous application of pCRP vs PC-pCRP. Western blot of native PAGE with 1/20th SDS stained for mCRP. pCRP solution and predissociated mCRP solution served as controls. A typical result of 3 experiments is shown. **D**, Immunohistochemical staining of the cremaster muscle with HistoGreen after treatment with LPS plus pCRP with or without PC. Clone 8D8 was used to detect pCRP and clone 9C9 to detect mCRP. Representative results are shown (n=6 for each sample). pCRP dissociation and interstitial deposition in LPS-triggered inflammation was abrogated by stabilization of pCRP with PC. **E**, Quantification of leukocyte-endothelium interaction in postcapillary venules of the inflamed cremasteric tissue by intravital microscopy under intravenous application of pCRP (25  $\mu$ g/mL) with or without PC by 20 minutes. Dot plots and mean of 6 rats are shown; # $P$ <0.05. By preventing CRP dissociation, PC masks the proinflammatory potential of CRP in acute inflammation and induces a significant decrease in leukocyte rolling after 60 minutes (**E**) and a significant decrease in leukocyte adhesion (**F**) after 120 minutes compared with the LPS+pCRP group. PC alone had neither proinflammatory nor anti-inflammatory potential. **G**, Flow chart of the intravital experimental protocol. **H**, Human mCRP but not pCRP was detected in infarcted rat myocardium after administration of human pCRP into the circulation. Noninfarcted right ventricular tissue from the same animal was used as a control and showed no (**Continued**)

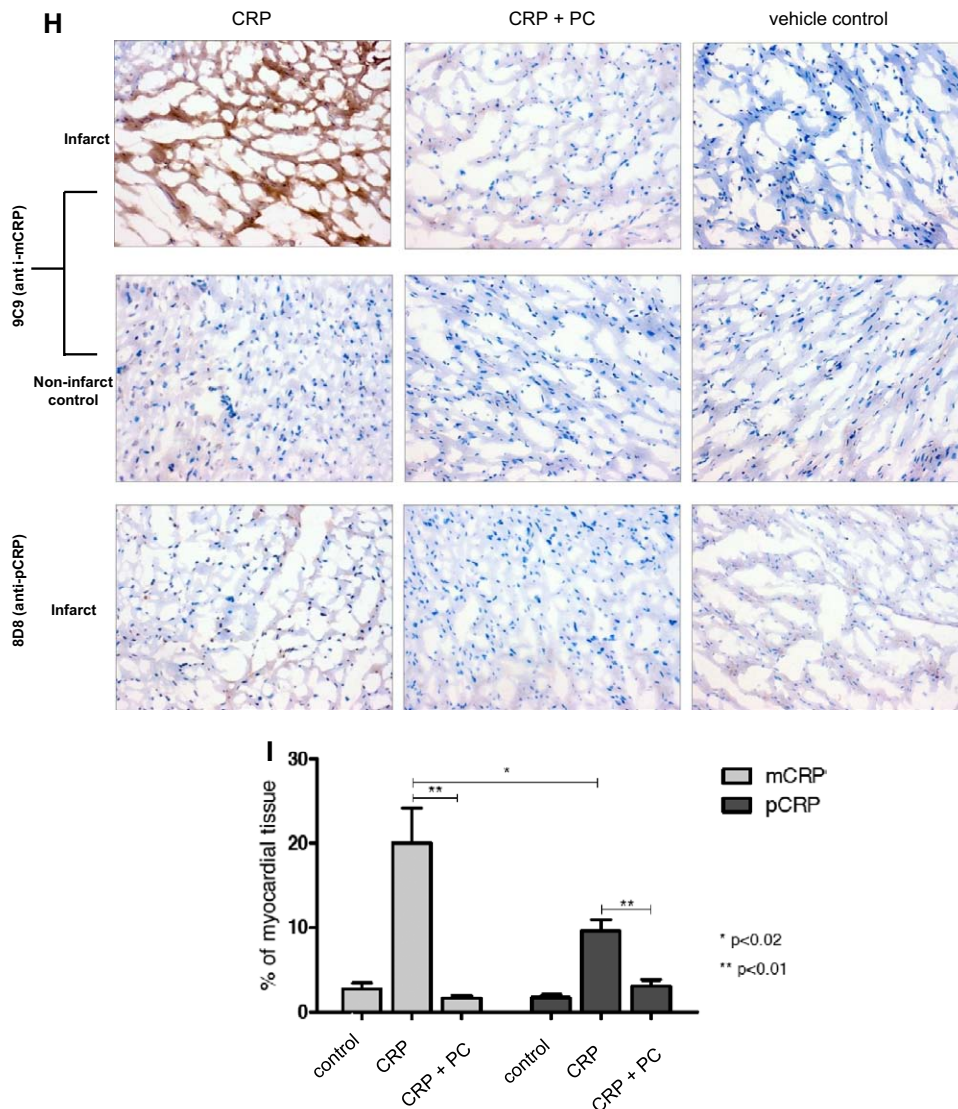


**Figure 7. Continued** evidence of mCRP or pCRP deposition. When pCRP was preincubated with PC (50:1 molar ratio), there was no significant deposition of mCRP or pCRP in either the infarcted or noninfarcted tissue. This result did not differ significantly from the vehicle control displayed in the third column.  $n=6$  rats per group; typical examples are given. I, Quantification of results shown in Figure 7H by use of image analysis software as described in Methods. Three slides of each animal were analyzed and averaged. The average counted as the value for 1 rat ( $n=6$ ).

after stabilization of CRP with 1,6-bis PC (Figure 7D). This blocking effect resulted in inhibition of the CRP-mediated increase in leukocyte rolling after 60 minutes and adhesion at 120 minutes (Figure 7E and 7F). This demonstrates the feasibility of this potential therapeutic approach and the central importance of pCRP dissociation in the unmasking of proinflammatory CRP effects.

### mCRP and pCRP Deposition Is Localized to Infarcted Myocardial Tissue in a Rat Model of Ischemia/Reperfusion Injury

To confirm the relevance of CRP dissociation in a disease model, we examined the proposed mechanism and its inhibition by 1,6-bis PC in a rat left anterior descending coronary artery ligation model of myocardial infarction. Histological examination of rat myocardium showed extensive deposition of mCRP in infarcted tissue, as shown in Figure 7H. In contrast, in noninfarcted right ventricular segments (Figure 7H,

row 2), no mCRP could be detected. Furthermore, control samples, which were not infused with human pCRP (Figure 7H, row 3), did not show any staining for mCRP. Small amounts of pCRP were detected in ischemic/reperfused tissue but in significantly lower amounts than mCRP. These findings were quantified by use of imaging analysis software, and the results are shown in Figure 7I. There was significantly more mCRP than pCRP identified in ischemic tissue segments. The non-ischemic and vehicle controls did not show specific staining.

### 1,6-bis-PC Inhibits the Formation and Deposition of mCRP in Infarcted Tissue and Reduces the Localized Inflammatory Response

In the myocardial ischemia/reperfusion model, a third experimental group was infused with human pCRP together with 1,6-bis-PC. This agent was able to completely abolish the formation and deposition of mCRP (Figure 7H). The amount of both mCRP and pCRP detected was not significantly

different from the vehicle and nonischemic controls, as shown in Figure 7I.

The reduced mCRP formation and deposition by 1,6-bis-PC led to a significant reduction of leukocyte infiltration, expression of caspase 3 (a marker of apoptosis), and expression of the proinflammatory cytokines interleukin 6 and tumor necrosis factor- $\alpha$  (which served as surrogate parameters for the degree of tissue injury) compared with the CRP control (Figure III in the online-only Data Supplement).

## Discussion

Here, we have identified and characterized the role of pCRP dissociation to mCRP for the first time in vivo in an animal model of acute inflammation. This points to the CRP dissociation process as a potential therapeutic target. This is supported by the following findings: (1) mCRP was detected in human tissue samples of inflamed striated muscle tissue, human atherosclerotic plaques, and areas of infarcted rat and human heart tissue and was typically colocalized with inflammatory cells. These findings are consistent with a ubiquitous causal role in inflammation. (2) CRP was deposited in inflamed or ischemic tissue but not in healthy tissue beds. It aggravated the preexisting inflammatory response by inducing pathological leukocyte-endothelium interaction and generation of reactive oxygen species. pCRP did not demonstrate any intrinsic inflammatory properties without preexisting inflammatory tissue damage. (3) CRP was deposited in the area of inflammation as mCRP. (4) Localized pCRP dissociation was dependent on PLA2-mediated endothelial membrane changes and exposure of LPC, which localized mCRP-induced inflammation to areas of PLA2 activation. The blocking of PLA2 by pharmacological inhibitors abrogated these membrane changes and resulted in inhibition of CRP dissociation and prevention of the proinflammatory effects of CRP in vivo. (5) mCRP had marked proinflammatory properties in vitro and in vivo. mCRP deposits in tissue promoted monocyte chemotaxis and recruited circulating leukocytes to areas of inflammation via Fc $\gamma$ -RI and Fc $\gamma$ -IIIa signaling. (6) mCRP was transported into inflamed tissue bound to transmigrating leukocytes. (7) 1,6-Bis-PC inhibited pCRP dissociation and inhibited CRP deposition in inflamed tissue. By preventing mCRP formation 1,6-bis-PC inhibited proinflammatory CRP effects in inflamed tissue. This hypothesis was confirmed in a rat model of myocardial infarction in which the therapeutic use of 1,6-bis-PC prevented localized mCRP formation and deposition within the infarcted tissue and in turn reduced the parameters of tissue injury and inflammation. (8) mCRP induced leukocyte rolling and adhesion via a complement-dependent mechanism. These results are summarized in the schematic drawing in Figure 8.

To verify the pathophysiological relevance of mCRP in vivo, we used a rat model, because even though rats have abundant CRP (300–600  $\mu$ g/mL in normal, healthy, pathogen-free rats), it does not activate rat complement.<sup>17</sup> This is in contrast to human CRP, which activates both rat and human complement but not mouse complement,<sup>18</sup> which is a major limitation to the use of mice in CRP research. Depletion of complement abrogated the effects of CRP,

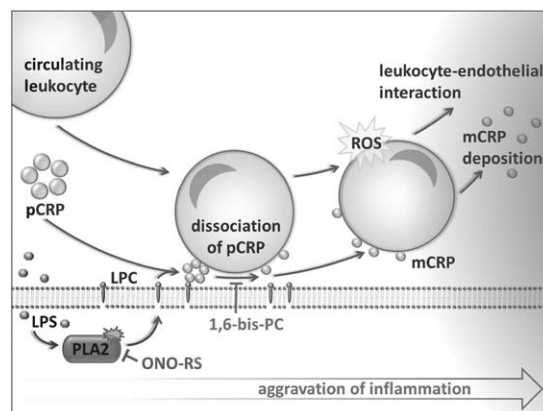


**Figure 8.** Proposed mechanism of phospholipase A2 (PLA2)-mediated lysophosphatidylcholine (LPC) generation and consecutive pentameric C-reactive protein (pCRP) dissociation in lipopolysaccharide (LPS)-induced inflammation. LPC mediates the dissociation of pCRP and is expressed on activated membranes via induction of PLA2. Monomeric subunit of C-reactive protein (mCRP) triggers leukocyte-endothelium interaction and is deposited in areas of inflammation. The proinflammatory effects of the resulting mCRP can be abrogated by inhibition of PLA2 with the PLA2 inhibitor ONO-RS and thus inhibition of LPS generation or by inhibition of pCRP dissociation by decameric stabilization of pCRP with 1,6-bis(phosphocholine) (1,6-bis-PC).

which confirms the crucial role that complement plays in CRP pathophysiology.<sup>6,7</sup>

One limitation of the use of rats is the limited availability of knockout animals. Therefore, we used a pharmacological approach to suppress PLA2 activity with a range of specific inhibitors to characterize its fundamental mechanistic role in CRP dissociation. However, this approach does not completely rule out the contribution of other unknown factors to the observed effects. Because PLA2 inhibition showed no effect on LPS-induced inflammation without the addition of pCRP, the present results show that PLA2 inhibition influences the effects of CRP-mediated exacerbation of inflammation. Further interpretations of the role of PLA2 in this context must be undertaken on the basis of the natural limitations of the experimental strategy, because the mechanism of the PLA2 inhibitors may be indirect or confounded by unidentified off-target effects.

To prove the ubiquitous character of the proinflammatory mechanism of localized pCRP dissociation, we analyzed mCRP in human infarcted myocardial tissue and in atherosclerotic plaques. In human myocardial tissue, pCRP could not be detected, which indicates that all bound pCRP underwent dissociation within hours of infarction. These findings were confirmed in a rat model of left anterior descending coronary artery ligation. The local deposition of mCRP was limited to areas of ischemic/necrotic tissue. In human atherosclerotic plaques, we showed that mCRP deposition was localized to the necrotic core of the lesion. Overall, these findings support the notion that CRP dissociation modulates inflammation in acute (cardiac ischemia/reperfusion) and chronic (atherosclerosis) inflammatory processes.

PLA2 enzymes are regulators of inflammation,<sup>11</sup> which is supported by the finding of reduced postischemic brain injury in a knockout mouse model deficient in cytosolic PLA2.<sup>19</sup>

Conversely, overexpression of Ca<sup>2+</sup>-independent PLA2-β led to increased vascular inflammation in a vascular ligation model in mice.<sup>20</sup> In addition to the release of arachidonic acid, activation of PLA2 results in the production of LPC. Generation of LPC via activation of the Ca<sup>2+</sup>-independent PLA2 and exposure of LPC on the cell surface is a mechanism generally identified in activated or apoptotic cells.<sup>21</sup> Lauber et al<sup>22</sup> identified Ca<sup>2+</sup>-independent PLA2 activation in apoptotic cells and subsequent LPC generation as a “find me” signal for macrophages. We visualized these membrane changes *in vivo* by expression of phosphatidylserine on endothelial cells detected by annexin V binding. Phosphatidylserine surface expression and LPC generation both are events in the early phase of cell damage<sup>23</sup> and present an “eat me” signal for macrophages.<sup>24</sup> Both phospholipids (phosphatidylserine and LPC) are central to the signaling pathways of apoptosis, and both are expressed on activated cell membranes and microparticles.<sup>25,26</sup> Thus, annexin V binding is a suitable parameter to monitor membrane changes and a suitable surrogate marker for the surface expression of LPC, because the expression of LPC and the expression of phosphatidylserine are concurrent events. For the first time, we were able to observe localized CRP dissociation *in vivo* by intravital imaging of the microcirculation of inflamed tissue by means of a specific fluorescently labeled anti-mCRP aptamer.<sup>16</sup> This localized mCRP generation was completely inhibited after PLA2 was blocked *in vivo*.

In the present experiments, LPS was used to activate PLA2<sup>27</sup> and facilitate LPC formation. This enabled the binding of circulating pCRP<sup>28</sup> and subsequent conformational changes of the protein.<sup>1,2</sup> The present findings complete the understanding of this inflammatory pathway. In addition to direct chemoattraction by LPC,<sup>22</sup> the conformational change of CRP is an activation signal to circulating leukocytes that marks the area of inflammation by localized deposition. These findings identify a novel mechanism by which PLA2 regulates inflammation.

Recently, a role for lipoprotein-associated, PLA2-generated LPC has been postulated for human atherosclerotic plaque formation.<sup>29</sup> We previously described the localized dissociation and deposition of mCRP in atherosclerotic plaques.<sup>1</sup> PLA2-mediated membrane changes and subsequent CRP dissociation may therefore be a ubiquitous mechanism in chronic inflammatory conditions such as atherosclerosis. This event is dependent on the expression of bioactive lipids, namely, LPC. In the present *in vivo* experiments, we showed that endothelial cells in inflamed areas underwent these membrane changes and were likely to be the mediators of CRP dissociation, whereas for our *in vitro* experiments, we used membrane changes of mononuclear cells to demonstrate the activity of PLA2 inhibitory agents and 1,6-bis PC on CRP dissociation, again demonstrating the ubiquity of this process. In our previous work, we demonstrated that activated platelet membranes could mediate this dissociation process in chronic inflammation.<sup>1</sup> Therefore, this mechanism is independent of the cell type and represents a general mechanism in various pathophysiological settings by which membrane changes caused by cell activation or apoptosis can activate an immune response via binding and dissociation of CRP, thereby resulting in leukocyte activation

and infiltration of the area of cellular damage. Our findings potentially link the novel mechanistic role of pCRP to mCRP dissociation with emerging data regarding an association of phospholipase activity and LPC generation with increased cardiovascular risk.<sup>30</sup>

In accordance with our previous data, the present findings do not indicate that pCRP possesses intrinsic proinflammatory potential, and CRP was not deposited outside areas of focal inflammation, which confirms the findings of a recent study in which pCRP infusions in healthy volunteers showed no proinflammatory effect.<sup>31</sup> The ability of CRP to mediate any inflammatory effects was dependent on a preexisting localized inflammatory microenvironment with PLA2-mediated membrane changes. In the clinical setting, this is reflected by the fact that levels of circulating pCRP rise 6 to 12 hours after the inflammatory insult.<sup>32</sup> This indicates that CRP dissociation is a modulator, in particular an amplifier, of an established inflammatory response rather than a first-line defense mechanism. Conversely, patients with a chronic mild elevation of circulating CRP levels have been found in numerous studies to be at increased cardiovascular risk.<sup>33</sup> In this setting, local dissociation of circulating pCRP in the inflamed intima of preatherosclerotic lesions might drive atherogenesis.

As a further proof for the relevance of the CRP dissociation process in aggravating the inflammatory response, the recently described compound 1,6-bis-PC was used. This agent acts by stabilizing CRP in a decameric form.<sup>5</sup> This stabilization prevents CRP dissociation *in vitro*.<sup>25</sup> We were able to show that the inhibition of pCRP dissociation by 1,6-bis-PC abolished the proinflammatory effects of CRP, a powerful inductive proof that demonstrates the relative importance of CRP in promoting innate immunity. The identification of this novel therapeutic approach may support the development of further compounds that are suitable for clinical use. However, it must be taken into consideration that the therapeutic inhibition of mCRP generation might reduce the proangiogenic effect of mCRP that has been described recently.<sup>34</sup> Inflammation as such is not necessarily harmful, but uncontrolled inflammation may be detrimental in conditions such as ischemia/reperfusion injury. Similarly, the proangiogenic effects of mCRP may be beneficial; however, in the context of an exaggerated inflammatory response, they may have less relevance. Therefore, targeting the effects of mCRP may be a valuable therapeutic strategy in these conditions.

Whereas the cremasteric muscle inflammation model served as a proof-of-concept model to identify the mechanism of CRP aggravated inflammation, we performed a rat left anterior descending coronary artery ligation model to confirm the relevance of this mechanism in a myocardial infarction. Previous animal models of myocardial infarction have found that CRP directly contributes to myocardial cell death and necrosis.<sup>5,7</sup> This finding is consistent with observational studies after myocardial infarction in humans, which have found that the peak serum (p)CRP level correlates with adverse clinical outcomes.<sup>35</sup> The mechanistic link establishing how CRP contributes to inflammation has been missing and is now elucidated by the present study. Histological studies have found that CRP and complement components (most often component C1q) can be found to be colocalized

in myocardial tissue during acute myocardial infarction.<sup>36</sup> We show that the depletion of serum complement abrogates any adverse effect of CRP, which strongly implies complement involvement in CRP pathogenesis. However, both pCRP and C1q are found independently in the plasma with no recognized interaction.<sup>37</sup> In contrast to pCRP, mCRP is a potent ligand of the complement component C1q.<sup>38</sup> The identification of an intermediate conversion step in the injured myocardial tissue is an elegant solution to these conflicting observations. The data obtained in our animal model supplement those previously published by Pepys et al,<sup>5</sup> because we have provided data to suggest that the mechanism of action of 1,6-bis-PC is to prevent mCRP formation by inhibiting pCRP binding and dissociation, which in turn reduces localized inflammation and tissue injury.

We conclude that in inflamed tissue, pCRP is dissociated, and the resulting mCRP is deposited and aggravates as well as localizes inflammatory responses such as leukocyte activation/infiltration. In inflammation, local membrane changes occur, and the present results indicate that these are induced by activation of PLA2 and subsequent exposure of bioactive lipids that mediate the conformational changes of pCRP. Therefore, the blocking of pCRP dissociation to a monomeric form or the inhibition of proinflammatory mCRP activity is a promising therapeutic strategy with the potential to offer a novel treatment approach in a wide range of inflammatory disorders.

### Acknowledgments

We acknowledge the invaluable assistance of Lila Adams of the CVPath Institute in the preparation and staining of the human myocardial infarct samples. We are grateful for expert statistical advice from Dr M. Olschewski and Prof. D. Hauschke, Institute for Medical Biometry and Medical Informatics, University of Freiburg.

### Sources of Funding

This work was supported by grants from the German Research Foundation to Dr Eisenhardt (EI 866/1-1 and EI 866/2-1) and the National Health and Medical Research Council of Australia and the Australian Research Council to Drs Habersberger and Peter.

### Disclosures

None.

### References

- Eisenhardt SU, Habersberger J, Murphy A, Chen YC, Woollard KJ, Bassler N, Qian H, von Zur Muhlen C, Hagemeyer CE, Ahrens I, Chindusting J, Bobik A, Peter K. Dissociation of pentameric to monomeric C-reactive protein on activated platelets localizes inflammation to atherosclerotic plaques. *Circ Res*. 2009;105:128–137.
- Ji SR, Wu Y, Zhu L, Potempa LA, Sheng FL, Lu W, Zhao J. Cell membranes and liposomes dissociate C-reactive protein (CRP) to form a new, biologically active structural intermediate: mCRP(m). *FASEB J*. 2007;21:284–294.
- Mihlan M, Blom AM, Kupreishvili K, Lauer N, Stelzner K, Bergström F, Niessen HW, Zipfel PF. Monomeric C-reactive protein modulates classic complement activation on necrotic cells. *FASEB J*. 2011;25:4198–4210.
- Eisenhardt SU, Thiele JR, Bannasch H, Stark GB, Peter K. C-reactive protein: how conformational changes influence inflammatory properties. *Cell Cycle*. 2009;8:3885–3892.
- Pepys MB, Hirschfield GM, Tennent GA, Gallimore JR, Kahan MC, Bellotti V, Hawkins PN, Myers RM, Smith MD, Polara A, Cobb AJ, Ley SV, Aquilina JA, Robinson CV, Sharif I, Gray GA, Sabin CA, Jenvey MC, Kolstoe SE, Thompson D, Wood SP. Targeting C-reactive protein for the treatment of cardiovascular disease. *Nature*. 2006;440:1217–1221.
- Hage FG, Oparil S, Xing D, Chen YF, McCrory MA, Szalai AJ. C-reactive protein-mediated vascular injury requires complement. *Arterioscler Thromb Vasc Biol*. 2010;30:1189–1195.
- Griselli M, Herbert J, Hutchinson WL, Taylor KM, Sohail M, Krausz T, Pepys MB. C-reactive protein and complement are important mediators of tissue damage in acute myocardial infarction. *J Exp Med*. 1999;190:1733–1740.
- Gill R, Kemp JA, Sabin C, Pepys MB. Human C-reactive protein increases cerebral infarct size after middle cerebral artery occlusion in adult rats. *J Cereb Blood Flow Metab*. 2004;24:1214–1218.
- Padilla ND, van Vliet AK, Schoots IG, Valls Seron M, Maas MA, Peltenburg EE, de Vries A, Niessen HW, Hack CE, van Gulik TM. C-reactive protein and natural IgM antibodies are activators of complement in a rat model of intestinal ischemia and reperfusion. *Surgery*. 2007;142:722–733.
- Malis CD, Bonventre JV. Mechanism of calcium potentiation of oxygen free radical injury to renal mitochondria: a model for post-ischemic and toxic mitochondrial damage. *J Biol Chem*. 1986;261:14201–14208.
- Teslenko V, Rogers M, Lefkowitz JB. Macrophage arachidonate release via both the cytosolic Ca<sup>2+</sup>-dependent and -independent phospholipases is necessary for cell spreading. *Biochim Biophys Acta*. 1997;1344:189–199.
- Smith PK, Krohn RI, Hermanson GT, Mallia AK, Gartner FH, Provenzano MD, Fujimoto EK, Goeke NM, Olson BJ, Klenk DC. Measurement of protein using bicinchoninic acid. *Anal Biochem*. 1985;150:76–85.
- Brown RE, Jarvis KL, Hyland KJ. Protein measurement using bicinchoninic acid: elimination of interfering substances. *Anal Biochem*. 1989;180:136–139.
- Khreiss T, József L, Hossain S, Chan JS, Potempa LA, Filep JG. Loss of pentameric symmetry of C-reactive protein is associated with delayed apoptosis of human neutrophils. *J Biol Chem*. 2002;277:40775–40781.
- Pepys MB, Hawkins PN, Kahan MC, Tennent GA, Gallimore JR, Graham D, Sabin CA, Zychlinsky A, de Diego J. Proinflammatory effects of bacterial recombinant human C-reactive protein are caused by contamination with bacterial products, not by C-reactive protein itself. *Circ Res*. 2005;97:e97–103.
- Wang MS, Black JC, Knowles MK, Reed SM. C-reactive protein (CRP) aptamer binds to monomeric but not pentameric form of CRP. *Anal Bioanal Chem*. 2011;401:1309–1318.
- de Beer FC, Baltz ML, Munn EA, Feinstein A, Taylor J, Bruton C, Clamp JR, Pepys MB. Isolation and characterization of C-reactive protein and serum amyloid P component in the rat. *Immunology*. 1982;45:55–70.
- Reifenberg K, Lehr HA, Baskal D, Wiese E, Schaefer SC, Black S, Samols D, Torzewski M, Lackner KJ, Husmann M, Blettner M, Bhakdi S. Role of C-reactive protein in atherogenesis: can the apolipoprotein E knockout mouse provide the answer? *Arterioscler Thromb Vasc Biol*. 2005;25:1641–1646.
- Bonventre JV. Roles of phospholipases A2 in brain cell and tissue injury associated with ischemia and excitotoxicity. *J Lipid Mediat Cell Signal*. 1997;17:71–79.
- Liu S, Xie Z, Zhao Q, Pang H, Turk J, Calderon L, Su W, Zhao G, Xu H, Gong MC, Guo Z. Smooth muscle-specific expression of calcium-independent phospholipase A2 $\beta$  (iPLA2 $\beta$ ) participates in the initiation and early progression of vascular inflammation and neointima formation. *J Biol Chem*. 2012;287:24739–24753.
- Kim SJ, Gershov D, Ma X, Brot N, Elkon KB. I-PLA(2) activation during apoptosis promotes the exposure of membrane lysophosphatidylcholine leading to binding by natural immunoglobulin M antibodies and complement activation. *J Exp Med*. 2002;196:655–665.
- Lauber K, Bohn E, Kröber SM, Xiao YJ, Blumenthal SG, Lindemann RK, Marini P, Wiedig C, Zobywalski A, Baksh S, Xu Y, Autenrieth IB, Schulze-Osthoff K, Belka C, Stuhler G, Wesselborg S. Apoptotic cells induce migration of phagocytes via caspase-3-mediated release of a lipid attraction signal. *Cell*. 2003;113:717–730.
- Balsinde J, Pérez R, Balboa MA. Calcium-independent phospholipase A2 and apoptosis. *Biochim Biophys Acta*. 2006;1761:1344–1350.
- Ravichandran KS, Lorenz U. Engulfment of apoptotic cells: signals for a good meal. *Nat Rev Immunol*. 2007;7:964–974.
- Habersberger J, Strang F, Scheichl A, Htun N, Bassler N, Merivirta RM, Diehl P, Krippner G, Meikle P, Eisenhardt SU, Meredith I, Peter K. Circulating microparticles generate and transport monomeric C-reactive protein in patients with myocardial infarction. *Cardiovasc Res*. 2012;96:64–72.

26. Ullal AJ, Pisetsky DS. The release of microparticles by Jurkat leukemia T cells treated with staurosporine and related kinase inhibitors to induce apoptosis. *Apoptosis*. 2010;15:586–596.
27. Yokote K, Morisaki N, Zenibayashi M, Ueda S, Kanzaki T, Saito Y, Yoshida S. The phospholipase-A2 reaction leads to increased monocyte adhesion of endothelial cells via the expression of adhesion molecules. *Eur J Biochem*. 1993;217:723–729.
28. Volanakis JE, Narkates AJ. Interaction of C-reactive protein with artificial phosphatidylcholine bilayers and complement. *J Immunol*. 1981;126:1820–1825.
29. Gonçalves I, Edsfieldt A, Ko NY, Grufman H, Berg K, Björkbacka H, Nitulescu M, Persson A, Nilsson M, Prehn C, Adamski J, Nilsson J. Evidence supporting a key role of Lp-PLA2-generated lysophosphatidylcholine in human atherosclerotic plaque inflammation. *Arterioscler Thromb Vasc Biol*. 2012;32:1505–1512.
30. Lavi S, McConnell JP, Rihal CS, Prasad A, Mathew V, Lerman LO, Lerman A. Local production of lipoprotein-associated phospholipase A2 and lysophosphatidylcholine in the coronary circulation: association with early coronary atherosclerosis and endothelial dysfunction in humans. *Circulation*. 2007;115:2715–2721.
31. Lane T, Wassef NL, Poole S, Mistry Y, Lachmann H, Gillmore J, Hawkins PN, Pepys MB. Infusion of pharmaceutical grade natural human C reactive protein is not proinflammatory in healthy adult human volunteers. *Circ Res*. 2013;114:672–676.
32. Gabay C, Kushner I. Acute-phase proteins and other systemic responses to inflammation. *N Engl J Med*. 1999;340:448–454.
33. Ridker PM, Buring JE, Shih J, Matias M, Hennekens CH. Prospective study of C-reactive protein and the risk of future cardiovascular events among apparently healthy women. *Circulation*. 1998;98:731–733.
34. Slevin M, Matou-Nasri S, Turu M, Luque A, Rovira N, Badimon L, Boluda S, Potempa L, Sanfeliu C, de Vera N, Krupinski J. Modified C-reactive protein is expressed by stroke neovessels and is a potent activator of angiogenesis *in vitro*. *Brain Pathol*. 2010;20:151–165.
35. Anzai T, Yoshikawa T, Shiraki H, Asakura Y, Akaishi M, Mitamura H, Ogawa S. C-reactive protein as a predictor of infarct expansion and cardiac rupture after a first Q-wave acute myocardial infarction. *Circulation*. 1997;96:778–784.
36. Lagrand WK, Niessen HW, Wolbink GJ, Jaspars LH, Visser CA, Verheugt FW, Meijer CJ, Hack CE. C-reactive protein colocalizes with complement in human hearts during acute myocardial infarction. *Circulation*. 1997;95:97–103.
37. Bíró A, Rovó Z, Papp D, Cervenak L, Varga L, Füst G, Thielens NM, Arlaud GJ, Prohászka Z. Studies on the interactions between C-reactive protein and complement proteins. *Immunology*. 2007;121:40–50.
38. Ji SR, Wu Y, Potempa LA, Liang YH, Zhao J. Effect of modified C-reactive protein on complement activation: a possible complement regulatory role of modified or monomeric C-reactive protein in atherosclerotic lesions. *Arterioscler Thromb Vasc Biol*. 2006;26:935–941.

### CLINICAL PERSPECTIVE

C-reactive protein (CRP) is an independent risk factor for cardiovascular events. Chronic mild elevations in serum CRP are associated with the progression of atherosclerosis. After myocardial infarction, the peak serum CRP correlates with adverse outcomes such as heart failure and death. Despite such strong associative studies, there has been considerable controversy as to whether elevated serum CRP is a causative factor in cardiovascular disease or merely correlates with atherosclerosis and myocardial infarction. Recently, we have shown that on binding to damaged cell membrane, pentameric (p) CRP can undergo dissociation to a proinflammatory, monomeric (m) CRP in a number of inflammatory settings. In this study, using both animal and human data, we show that CRP undergoes dissociation at sites of inflammation, including striated and cardiac muscle, as well as at atherosclerotic plaques. This process is dependent on the action of phospholipase A2, which generates lysophosphatidylcholine on membrane surfaces. This enables pCRP binding and its dissociation to mCRP, which then is deposited and via its proinflammatory effects acts to amplify and localize inflammation, contributing to aggravation of tissue damage. Most important, we show that blocking pCRP dissociation, either by preventing the aforementioned membrane changes by inhibition of phospholipase A2 or by inhibiting CRP dissociation by the compound 1,6-bis(phosphocholine)-hexane, prevents detrimental proinflammatory CRP effects. Therefore, we identified the blocking of pCRP dissociation to mCRP and thereby the prevention of proinflammatory mCRP activity as a promising therapeutic strategy that offers the potential of a novel treatment approach in a wide range of inflammatory disorders, including atherosclerosis and myocardial infarction.



**Dissociation of Pentameric to Monomeric C-Reactive Protein Localizes and Aggravates Inflammation: In Vivo Proof of a Powerful Proinflammatory Mechanism and a New Anti-Inflammatory Strategy**

Jan R. Thiele, Jonathon Habersberger, David Braig, Yvonne Schmidt, Kurt Goerendt, Valentin Maurer, Holger Bannasch, Amelie Scheichl, Kevin J. Woollard, Ernst von Dobschütz, Frank Kolodgie, Renu Virmani, G. Bjoern Stark, Karlheinz Peter and Steffen U. Eisenhardt

*Circulation*. 2014;130:35-50; originally published online April 28, 2014;  
doi: 10.1161/CIRCULATIONAHA.113.007124

*Circulation* is published by the American Heart Association, 7272 Greenville Avenue, Dallas, TX 75231  
Copyright © 2014 American Heart Association, Inc. All rights reserved.  
Print ISSN: 0009-7322. Online ISSN: 1524-4539

The online version of this article, along with updated information and services, is located on the World Wide Web at:

<http://circ.ahajournals.org/content/130/1/35>

Data Supplement (unedited) at:

<http://circ.ahajournals.org/content/suppl/2014/04/28/CIRCULATIONAHA.113.007124.DC1.html>

**Permissions:** Requests for permissions to reproduce figures, tables, or portions of articles originally published in *Circulation* can be obtained via RightsLink, a service of the Copyright Clearance Center, not the Editorial Office. Once the online version of the published article for which permission is being requested is located, click Request Permissions in the middle column of the Web page under Services. Further information about this process is available in the [Permissions and Rights Question and Answer](#) document.

**Reprints:** Information about reprints can be found online at:  
<http://www.lww.com/reprints>

**Subscriptions:** Information about subscribing to *Circulation* is online at:  
<http://circ.ahajournals.org/subscriptions/>

## **Supplemental Material**

### **Methods**

#### *Reagents*

The anti-pCRP antibody clone 8D8 and anti-mCRP antibody clone 9C9 were generated and characterized for conformation-specificity as described<sup>16</sup> and used as hybridoma supernatant. The aforementioned reagents were kindly provided by Dr. Larry Potempa (College of Pharmacy, Roosevelt University, Schaumburg, USA). Anti-CRP antibody clone 8, Lipopolysaccharide from *Escherichia coli* serotype O127:B8 (LPS), phosphatase substrate, MAFP (methyl Arachidonyl fluorophosphonate) and ONO-RS-082 were all obtained from Sigma-Aldrich. Alexa488 labeled Annexin V solution was obtained from Life Technologies (Carlsbad, USA), mouse anti-human CD68 from Dako. mCRP binding RNA aptamer was purchased from Integrated DNA Technologies (Leuven, Belgium), and labeled with Alexa488. The aptamer sequence was: 5'-Alexa488-GCC UGU AAG GUG GUC GGU GUG GCG AGU GUG UUA GGA GAG AUU GC-3'<sup>1</sup>. Stocks were reconstituted with DEPC-treated water and stored at -20°C until used. Cobra venom factor (CVF) was obtained from Quidel (Santa Clara, USA) and stored at -70°C until use. 1,6-bis(phosphocholine)-hexane (PC) was synthesized by Syngene International, Bangalore, India.

#### *Immunohistology of human tissue samples*

Tissue samples were obtained from 11 patients receiving reconstruction of soft tissue defects after traumatic injuries of the lower extremity by means of free muscle transfer as described previously<sup>2</sup>. The first sample was taken intra-operatively

immediately prior to interruption of the blood supply and the second one after ischemia and reperfusion on post-operative day 5. The study was approved by the ethic committee of the University of Freiburg Medical Centre and informed consent was obtained from each patient. Immunohistological staining and analysis by planimetry were performed according to previously published protocols <sup>2,3</sup>. Antibody clone 8D8 was used for the detection of pCRP and clone 9C9 for the detection of mCRP <sup>4</sup>.

Human atherosclerotic plaques derived from carotid endarterectomy were stained as described above. After incubation with HRP-labeled anti-mouse antibody (Dako, Glostrup, Denmark) reaction products were stained with HistoGreen substrate kit for peroxidase (Linaris, Dossenheim, Germany) resulting in a green reaction product.

For staining of human myocardial tissue samples were obtained from the CVPPath Institute (Gaithersburg, Maryland, USA). All samples had been referred for post-mortem examination and cases where myocardial infarction had been determined to occur between 2 and 5 days prior to death were selected. Myocardial tissue was fixed in formalin prior to examination and histology was performed as described previously<sup>3</sup>.

Samples were prepared as described previously <sup>5</sup> with slight modification. Slides were de-parafinized in xylene and rehydrated in graded alcohol solutions followed by distilled water. Antigen retrieval was performed by 30 min of heating at 37°C in 2M hydrochloric acid solution. Samples were rinsed and the staining protocol continued as published previously <sup>5</sup>.

*Animal model for intravital microscopy studies*

Animal studies were approved by the institutional animal care committee of the University of Freiburg, Germany. Male Wistar rats (Charles River, Sulzfeld, Germany) weighing 120 - 180 g were used. A detailed protocol has been previously described <sup>6</sup>. Leukocyte-endothelial interactions in the cremaster muscle were observed by intravital microscopy. Leukocytes were labeled by intravenous injection of rhodamine 6G (0.4 mg/kg body weight, Sigma-Aldrich) <sup>7</sup>. Leukocytes were considered adherent to the endothelium if they remained stationary for 20 s or more. Rolling leukocytes were defined as those moving at a velocity less than that of erythrocytes within a given vessel. One to three postcapillary venules with a diameter of 20 - 50  $\mu\text{m}$  were chosen for observation; to minimize variability, the same section of cremasteric venule was observed throughout the experiment.

Following stabilization of the tissue, a recording of 30 seconds was made to establish baseline values for leukocyte rolling and adherence. To minimize the influence of pre-activation of the tissue, only vessels in which leukocyte rolling was <20 cells/30 seconds and the number of adherent cells <10 cells/200  $\mu\text{m}$  of endothelium were utilized for study. Animals observed over a 120 min protocol were randomly assigned to 8 different groups as follows (n=6 for each group). LPS: The cremaster muscle was constantly superfused with low dose (25 ng/ml) LPS for 120 min. Control: vehicle control (PBS-Ca-Mg). pCRP: A pCRP-solution bolus (25  $\mu\text{g}/\text{ml}$  serum concentration) was injected at 20 min. Weight-dependent rat serum volume was calculated <sup>8</sup> and serum levels were verified by a particle-enhanced immunoturbidimetric assay (Modular Analytics, Roche Diagnostics, Basel, Switzerland). LPS+pCRP: pCRP was injected after 20 min (at 25  $\mu\text{g}/\text{ml}$  serum concentration) in addition to the superfusion with LPS (25 ng/ml). In some groups, we added ONO-RS-082 (ONO) at 10  $\mu\text{M}$  to the superfused solution for reversible PLA 2 blockade. Superfusion was initiated at 0 min. For decameric stabilization 1 mg/ml

pCRP solution was incubated with 1,6-bis(Phosphocholine)-hexane (PC) in 100 to 1 molar ratio for 30 min at 37°C. Animals observed over a 60 min protocol and were randomly assigned to 4 different groups (n=6 for each group). pCRP and mCRP were both injected at 25 µg/ml serum concentration after establishing baseline values of leukocyte rolling and adhesion. Constant superfusion with LPS (1 µg/ml) served as a positive control and PBS-CA-Mg as vehicle control.

To investigate the role of the complement system in CRP mediated inflammation *in vivo*, rats were treated with CVF (250 U/kg bodyweight) 24 hours before intravital imaging via i.p. injection<sup>9</sup>. Deactivation of the hemolytic complement activity in rat serum was measured by calculation from the dilution producing 50% lysis of optimally sensitized sheep erythrocytes using the CH 50 test from Diamedix (Miami, USA).

#### *Rat myocardial infarction/reperfusion model, histology and quantitative PCR*

Adult male Wistar rats were weighed and anaesthetized. Following a sub-costal incision the left anterior descending coronary artery was ligated with a quick release suture. Myocardial ischemia was confirmed via electrocardiograph changes and myocardial pallor. Lignocaine 1mg/kg was administered intravenously to minimize electrical instability. After 40 min of ischemia the coronary suture was released and human CRP (200 µg), human CRP incubated with PC (200 µg CRP, 50:1 molar ratio PC:CRP) or vehicle control were infused intravenously. Animals remained anaesthetized and were sacrificed after a further hour by exsanguination. The hearts were excised, suspended in OCT compound and fresh frozen in liquid nitrogen prior to storage at -80°C. All experiments were approved by and performed in accordance with the institutional animal ethics committee.

6µm fresh frozen sections were analyzed by immunohistochemistry with conformation-specific anti-CRP antibodies as described above. Histological analysis was performed on infarcted and non-infarcted myocardium. Infarcted areas were identified anatomically from the left anterior descending artery territory. Right ventricular free wall tissue supplied by the non-ligated right coronary artery was used as a matched non-ischemic control in all samples reported. For determination of myocardial damage, sections were stained with Alexa 488 anti-rat CD45 antibody (1:50 dilution, Biolegend). Vascular margins were displayed via Cy3-conjugated monoclonal anti  $\alpha$ -smooth muscle actin (SMA) antibody clone 1A4 (1:200 dilution, Sigma-Aldrich). The number of leukocytes in tissue was quantified in at least three non-overlapping visual fields of each sample to determine the corresponding value (n=3). Nuclei were stained blue with DAPI mounting medium (Vector Laboratories). For determination of CRP deposition, Alexa 488 labeled clone 8 antibody (Sigma-Aldrich) was used in a 1:100 dilution. Analysis was carried out by planimetry. For the quantification of mRNA-expression, 30mg frozen infarcted and non-infarcted myocardium was disintegrated and homogenized mechanically by using the Ultra-Turrax (IKA-Werke, Staufen, Germany). The RNA isolation was done by RNeasy Fibrous Tissue Mini Kit (Quiagen). RNA was dissolved in 30µl RNase-free water and concentration and purity of RNA were determined spectrophotometrically. cDNA synthesis and TaqMan PCR assays were performed as described under "Fcγ-Receptor studies". Rat-specific primers and probes were obtained from Applied Biosystems (Primerset Caspase 3, Primerset IL-6, Primerset TNF; TaqMan Gene Expression Assays). Data were analyzed using the relative standard curve method, with each sample being normalized to GAPDH.

### *In vivo Phosphatidylserine detection*

Alexa488 labeled Annexin V solution (Life Technologies) was intravenously injected in male Wistar rats at 1 ml/kg BW. Cremasteric superfusion with LPS (25 ng/ml) was initiated 20 min later. Endothelial associated phosphatidylserine expression in the cremaster muscle was detected via Annexin V specific binding as previously described<sup>10</sup>. The fluorescence signal was measured by digital intravital epifluorescence microscopy in 20 min intervals (n=3).

### *In vivo pCRP tracking and mCRP detection*

For some intravital experiments, pCRP was fluorescently labeled with Alexa594 according to the manufacturer's protocol (Protein Labeling Kit, Life Technologies) to form stable dye-protein conjugates (L-pCRP).

For the detection of mCRP Alexa488 labeled mCRP binding aptamer (mCRP-Apt.) was intravenously injected (2.5 µg/ml serum concentration) 100 min after LPS superfusion (25 ng/ml) and application of L-pCRP (25 µg/ml) as previously described in the presence or absence of ONO (10 µM). The fluorescence signal was assessed after 120 min (n=3). For *in vitro* testing a collagen matrix was coated with pCRP and mCRP (25 µg/ml) followed by incubation at 4°C overnight. Blockade with 1% BSA was followed by addition mCRP-Apt. for 1 hour at RT at various concentrations. After extensive washing against PBS-Ca-Mg aptamer binding was quantified using fluorescence spectroscopy.

Pro-inflammatory testing of mCRP-Apt. was conducted in a static monocyte adhesion assay described below in the presence or absence of mCRP-Apt. at 1 and 5 µg/ml.

### *Measurement of ROS generation*

After intravital microscopy rats were killed by exsanguination. Mononuclear cells were isolated from whole blood by Ficoll density gradient centrifugation. ROS formation was determined by electron spin resonance spectroscopy (ESR) using CMH (1 mM, 1-hydroxy-3-methoxycarbonyl-2,2,5,5-tetramethylpyrrolidine, Noxygen, Elzach, Germany) as the spin label and was prepared as described by Kuzkaya et al.<sup>11</sup>. Cell count was determined and 500 µl of cell suspension were incubated at 37°C for 30 min with 25 µg/ml CMH (1 mM). The oxidation of spin probe CMH by ROS generated stable 3-methoxycarbonyl-proxyl radicals (CM<sup>•</sup>)<sup>12</sup> was quantified by ESR referring to standard CM<sup>•</sup> solutions. Measurements were performed using a MiniScope MS 200 ESR Spectrometer (Magnettech, Berlin, Germany) with following instrument settings: center field, 3340 G; sweep wide, 60 G; sweep time, 5 milliseconds over 10 scans; modulation amplitude, 2.4 G; microwave power, 10 mW. Results were charged against the cell concentration and expressed as percentage of values of the control group.

### *Experimental protocol of the Fcγ-receptor studies*

Monocytes were isolated from peripheral venous blood of healthy human volunteers and cultured for 24 hours (37°C / 5% CO<sub>2</sub>). After transfection with the respective siRNA cells were harvested, centrifuged and TaqMan RT-PCR was performed. Total RNA was prepared using the RNeasy Mini Kit (Qiagen, Hilden, Germany) following the manufacturer's instructions. Total RNA (0.5 µg) was treated with 3 units of desoxyribonuclease I (DNase I, Invitrogen, Karlsruhe, Germany) to digest genomic



DNA contamination. Random-primed cDNA synthesis was performed using 0.5 µg of DNase I-treated total RNA and 50 units of AffinityScript reverse transcriptase according to the manufacturer's instructions (Stratagene, La Jolla, USA). TaqMan PCR assays were performed in 384-well optical plates on a LightCycler (Roche, Mannheim, Germany) using Absolute qPCR ROX Mix (Abgene, Hamburg, Germany) according to the manufacturer's instructions. Oligonucleotide primers and probes for human GAPDH (GAPDH Forward Primer, GAPDH-875F; GAPDH Reverse Primer, GAPDH-946R; GAPDH-probe-899; Eurofins MWG Operon, Ebersberg, Germany), human Fc $\gamma$ -Receptor I (Primerset Fc $\gamma$ -RI, TaqMan Gene Expression Assays, Applied Biosystems, Foster City, USA), IIA (Primerset Fc $\gamma$ -RIIA, TaqMan Gene Expression Assays), IIIA (Primerset Fc $\gamma$ -RIIIA, TaqMan Gene Expression Assays) were used. Data were analyzed using the relative standard curve method, with each sample being normalized to GAPDH to correct for differences in RNA quality and quantity.

### *Flow cytometry*

Transfected cells were harvested, cleaned and the pellet was resuspended in PBS + 2% FCS. For each sample tubes (BD Falcon 5ml Polystyrene Round-Bottom Tube, BD Biosciences) were prepared containing 100 µl cell suspension and 5 µl FITC-labeled antibody (Monoclonal anti-human CD16, Clone 3G8, Sigma-Aldrich; Anti-Human CD32-FITC, Clone IV.3, Stemcell Technologies, Grenoble, France; Human CD64 FITC Conjugate Mouse IgG1, Invitrogen) or 5 µl FITC-labeled isotype control antibody (IgG1-FITC Isotype Control, Clone MOPC 21, Sigma-Aldrich; FITC Mouse IgG2b, Clone MPC-11, BioLegend, San Diego, USA; Mouse IgG1 FITC Conjugate Negative Control, Invitrogen), respectively. After an incubation period of 30 min, 1 ml

of PBS +2 % FCS was added and flow cytometry was performed using BD LSRFortessa Cell Analyzer (BD Biosciences).

#### *Immunohistology of rat cremasteric tissue*

After intravital microscopy the cremaster muscle was excised, placed in tissue freezing medium (Leica Microsystems, Nussloch, Germany), and stored at -20°C. Specimens were cut vertically into 6 µm thick serial sections and immobilized on pre-cleaned microscope slides (SuperFrost, R. Langenbrinck, Emmendingen, Germany). Anti-macrophage/monocyte antibody clone ED-1 (Millipore, Billerica, USA) was used in a 1:100 dilution to bind transmigrating rat monocytes/macrophages and fluorescently detected with FITC-anti-mouse secondary antibody (1:1000 dilution, Sigma-Aldrich). Venule margins were displayed via Cy3 conjugated monoclonal anti  $\alpha$ -smooth muscle actin (SMA) antibody clone 1A4 (1:200 dilution, Sigma-Aldrich). Macrophages/monocytes level with the  $\alpha$ -SMA<sup>+</sup> layer or beyond within a 50 µm distance were regarded as transmigrated. At least 9 venules of 50-150 µm in diameter were quantified per rat at non-overlapping levels (n=3). Nuclei were stained blue with DAPI mounting medium (Vector Laboratories, Burlingame, USA). For detection of CRP specimens were cut horizontally. Staining was performed as described previously<sup>3</sup>. Antibody clone 8D8 was used for the detection of pCRP and 9C9 for the detection of mCRP. Analysis was carried out by planimetry.

#### *Static monocyte adhesion assay*

Static monocyte adhesion assays were conducted as previously described<sup>13</sup>. Briefly, monocytes from healthy human volunteers or from male Wistar rats were purified by

Ficoll gradient centrifugation ( $1 \times 10^6$ /ml) and incubated with either forms of CRP at 25  $\mu$ g/ml for 60 min at 37°C. mCRP-Apt was added at 1 or 5  $\mu$ g/ml to the CRP isoforms. 100  $\mu$ l/well of this suspension was added to fibrinogen coated 96-well plates (Nunc MaxiSorp®, Sigma-Aldrich) in triplicates and allowed to adhere for 60 min. After extensive washing with PBS-Ca-Mg phosphatase substrate stain (50 mM sodium acetate pH 5.0, 1% Triton X-100 and 6 mg/ml of phosphatase substrate, all from Sigma) was added and incubated for 1 h at 37°C. Staining was terminated with 1 M NaOH and absorbance measured at 405 nm by spectrophotometry. Monocytes incubated with 25  $\mu$ g/ml LPS served as positive control.

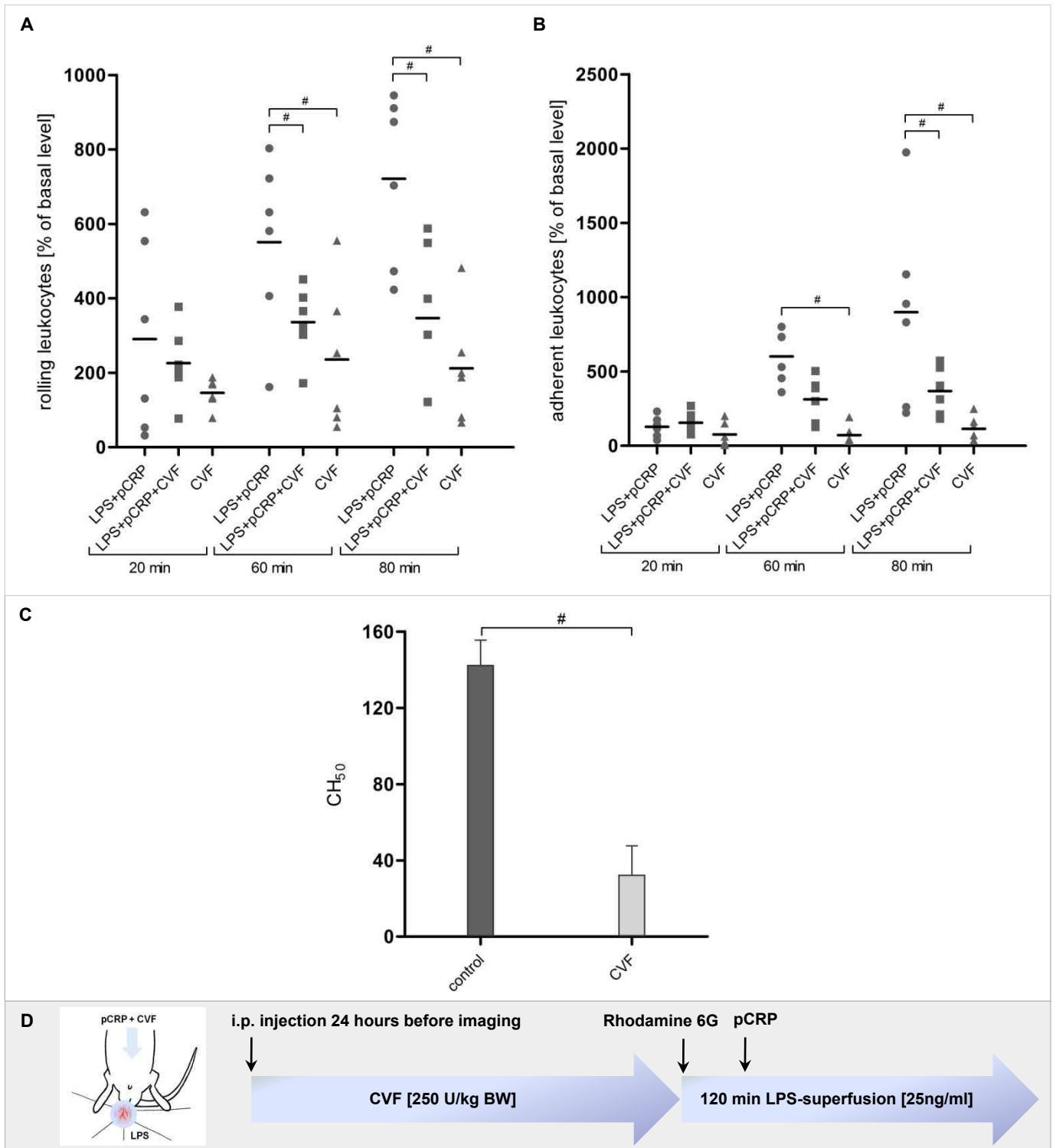
#### *Determination of PLA<sub>2</sub> activity*

Phospholipase A<sub>2</sub> activity in lysates of mononuclear leukocytes was assayed by EnzChek Phospholipase A<sub>2</sub> Assay Kit (Invitrogen). Briefly, freshly isolated human mononuclear leukocytes ( $2 \times 10^6$ /ml in RPMI 1640 medium) were incubated with PLA<sub>2</sub> inhibitor ONO-RS (10 mM) for 30 min followed by LPS (25 ng/ml) for 2 h at 37° C. Cells were washed in PBS and resuspended in 200 $\mu$ l PLA<sub>2</sub> assay buffer. Cell lysis was accomplished by repeated freezing and thawing in liquid nitrogen and pressing the lysate through a 27G needle. Lysates were cleared of cell debris by centrifugation and the protein concentration was adjusted to 4mg/ml. PLA<sub>2</sub> activity was measured by the intensity increase of a single wavelength at 515nm according to the manufacturer's protocol.

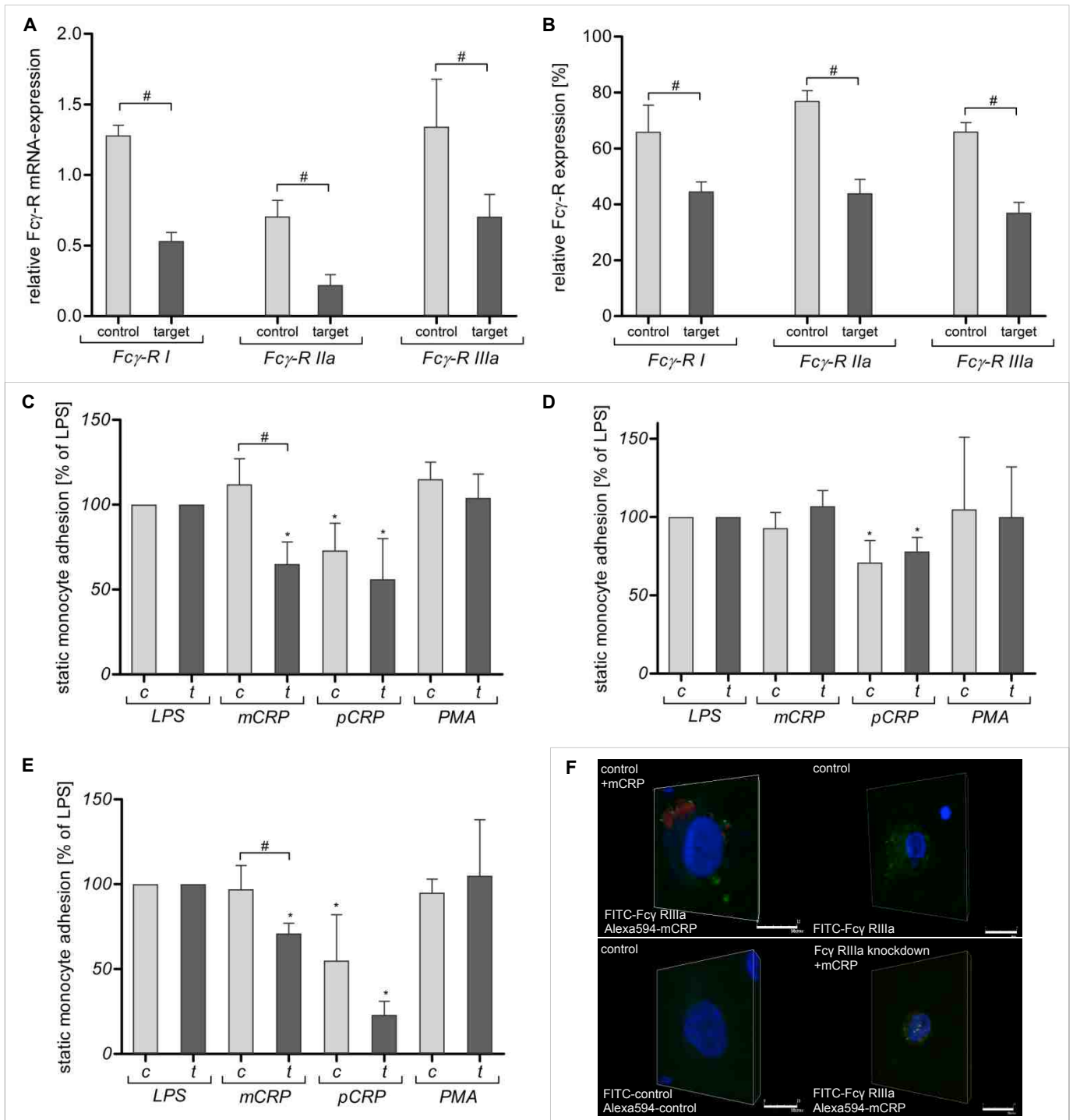
#### *Western blot analysis*

For CRP detection in rats, tissue was homogenized on ice using an ultra turrax (Ika, Staufen, Germany). Cells from rat tissue or rat monocytes were lysed by addition of lysis buffer (1 % NP-40, 0.5% sodiumdeoxycholate, 0.1% sodium dodecyl sulfate (SDS), 0.2 mM phenylmethylsulfonyl fluoride, 1 µg/ml aprotinin, 1 µg/ml leupeptin, and 1 mM sodium orthovanadate). Particulate material was removed by centrifugation and protein concentration of the supernatants was determined using a BCA protein assay kit (Sigma-Aldrich). About 20 µg of total protein were separated by SDS gel electrophoresis, transferred to Hybond ECL nitrocellulose membranes (GE Healthcare, Munich, Germany), and probed with anti-CRP antibodies for 1 h at RT. To confirm equal loading of the gel, the membrane was stripped and re-probed with monoclonal antibodies against β-actin (Sigma-Aldrich) or GAPDH (abcam, Cambridge, UK). Detection was performed after incubation of the membrane with an anti-mouse horseradish peroxidase-conjugated secondary antibody (Dianova, Hamburg, Germany) for 1 h at RT using enhanced chemiluminescence (ECL, GE Healthcare) as described by the manufacturer and captured on Hyperfilm ECL (GE Healthcare). The signal intensity per millimeter squared was quantified by ImageJ version 1.46 (background values were subtracted). For Western blotting with SDS reduced to 1/20<sup>th</sup> of normal levels cell lysis buffer containing 20mM Bis(2-hydroxyethyl)amino-tris(hydroxymethyl)methane, 500 mM ε-aminocaproic acid, 20 mM NaCl, 10% glycerol, 0,5% Triton, and protease inhibitors were used. SDS levels in all solutions were reduced to 1/20<sup>th</sup> of normal levels (0,4% SDS in sample buffer). Buffers were produced without Dithiothreitol (DTT) and β-Mercaptoethanol.

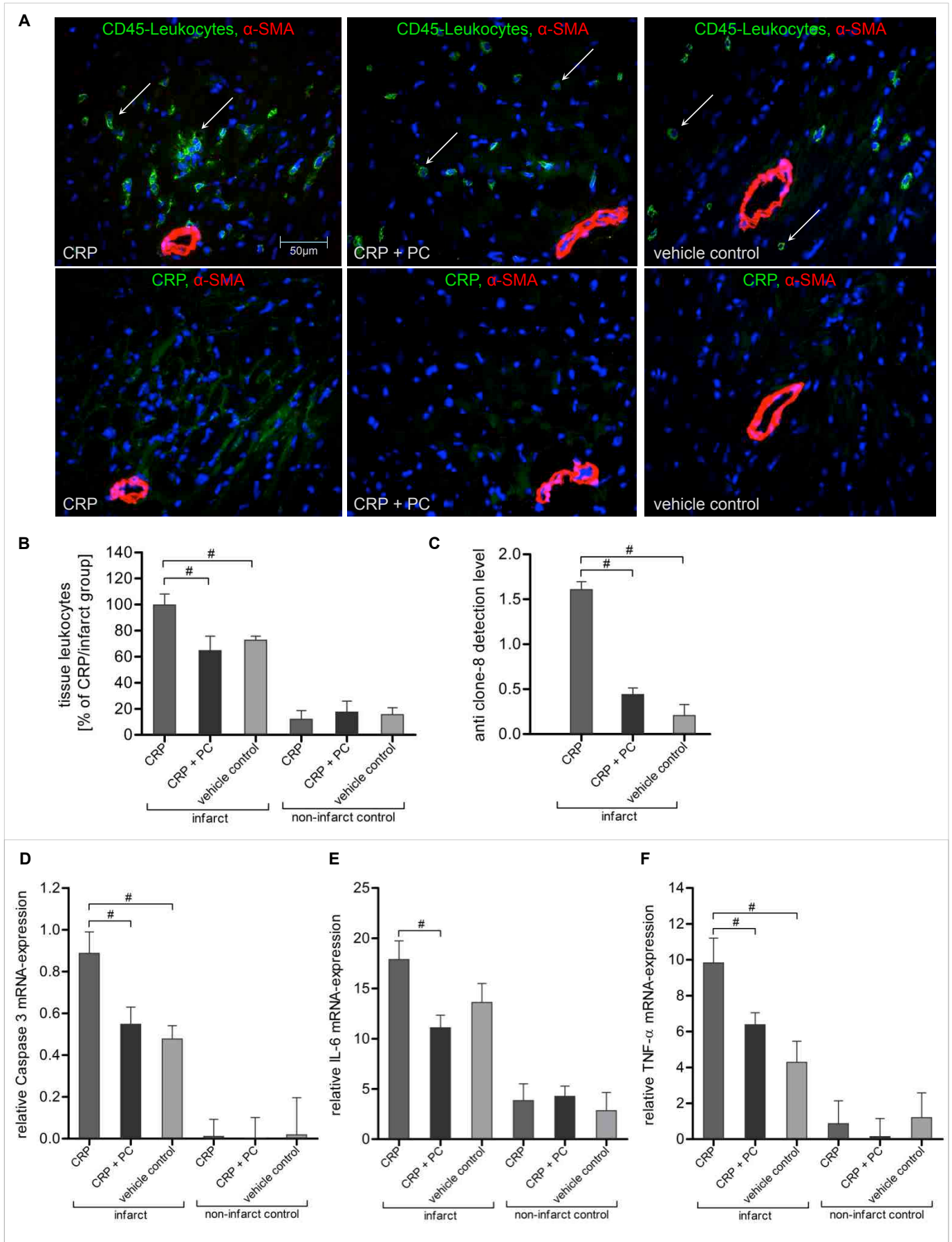
Online Supplemental Figure 1



Online Supplemental Figure 2



Online Supplemental Figure 3



## Online Supplemental Figure Legends

### Supplemental Figure 1

(A) Prevention of CRP-mediated inflammation by depletion of the complement system. Leukocyte-endothelial interaction under superfusion with LPS (25 ng/ml)  $\pm$  i.v. application of pCRP (25  $\mu$ g/ml) in complement-depleted rats quantified by intravital microscopy. Dot plots and mean of 6 rats are shown; #  $p < 0.05$ . Depletion of the complement system via i.p. injection of CVF (250 U/kg BW) 24 hours prior to intravital imaging prevents the CRP-induced pro-inflammatory potential on circulating leukocytes in LPS-triggered inflammation with a significant decrease of leukocyte rolling after 60 min (A) and adhesion (B) at 120 min. (C) Quantification of the complement system activity by measuring the 50% hemolytic complement (CH50) activity of rat serum. Experiments were performed in triplicates. Mean  $\pm$  SEM are given. #  $p < 0.05$ . Application of CVF at 250 U/kg BW induces a significant decrease in complement system activity 24 hours after i.p. injection (n=3 rats). (D) Flow chart of the intravital experimental protocol.

### Supplemental Figure 2

(A,B) Fc $\gamma$  receptor knockdown in human monocytes evaluated on mRNA and protein expression level. (A) Fc $\gamma$ -R mRNA-expression is significantly lower in all knockdown groups. (B) Quantification of Fc $\gamma$ -R surface-expression via flow cytometry shows an equivalent reduction after Fc $\gamma$ -R-knockdown. #  $p < 0.05$ ; values are mean  $\pm$  SEM (n=3). (C-E) Results of static monocyte adhesion assays under Fc $\gamma$ -RI (C), Fc $\gamma$ -RIIA (D) and Fc $\gamma$ -RIIIA (E) knockdown. Receptor knockdown results in a significant reduction of the pro-inflammatory potential of mCRP for Fc $\gamma$ -RI and Fc $\gamma$ -RIII, whereas Fc $\gamma$ -RIIA knockdown has no significant effect. #  $p < 0.05$ ; \* indicates a



$p < 0.05$  compared to the corresponding LPS control ( $n=3$ ). (F) Fc $\gamma$ -RIIIa knockdown reduces mCRP binding to monocytes. Addition of mCRP leads to receptor clustering and Fc $\gamma$ -RIIIa co-localization with mCRP in native monocytes. Fc $\gamma$ -RIIIa expression on monocytes was visualized by FITC labeled anti-Fc $\gamma$ -RIIIa antibody. mCRP binding was visualized with Alexa594 labeled anti-CRP antibody (clone 8). FITC and Alexa Fluor594 isotype control show no binding. Representative results of confocal microscopy are shown.

### Supplemental Figure 3

Stabilization of pCRP with 1,6-bis PC prior to i.v. application in rats prevents the CRP-induced tissue damage in infarcted myocardium. (A) Immunofluorescence detection of tissue leukocytes in rat myocardium using Alexa488-anti CD45 antibody (upper panel) and detection of CRP (lower panel) using Alexa488-clone 8 antibody. Vascular margins are displayed via Cy3-anti  $\alpha$ -SMA stain, nuclei are stained with DAPI. Representative results of the infarcted myocardium are shown. (B,C) Quantification of the immunofluorescence results. (B) Mean leukocyte count of the CRP group in infarcted tissue was set to 100%; #  $p < 0.05$ . (C) Relative values of immunofluorescence for CRP are shown. At least three non-overlapping visual fields were evaluated of each sample to determine the corresponding value.  $n=3$  rats / group; #  $p < 0.05$ . Values are mean  $\pm$  SEM. Addition of 1,6-bis PC prevents deposition of CRP and significantly decreases the number of leukocytes in the infarct, which were increased in number under i.v. application of CRP alone. (D-F) Relative mRNA expression of Caspase 3, IL-6 and TNF- $\alpha$  in infarcted rat myocardium and non-infarcted myocardium. Values were normalized to GAPDH to correct for differences in RNA quality and quantity.  $n=3$  rats / group; #  $p < 0.05$ . Values are mean  $\pm$  SEM.

CRP significantly increases the expression of Caspase 3 and TNF- $\alpha$  in infarcted tissue. IL-6 induction under CRP does not reach statistical significance compared to the vehicle control. 1,6-bis PC prevents the CRP-induced tissue damage in myocardial infarction and significantly decreases Caspase 3, TNF- $\alpha$  and IL-6 expression.

## References

1. Wang MS, Black JC, Knowles MK, Reed SM. C-reactive protein (crp) aptamer binds to monomeric but not pentameric form of crp. *Anal Bioanal Chem*. 2011;401:1309-1318
2. Eisenhardt SU, Schmidt Y, Karaxha G, Iblher N, Penna V, Torio-Padron N, Stark GB, Bannasch H. Monitoring molecular changes induced by ischemia/reperfusion in human free muscle flap tissue samples. *Annals of plastic surgery*. 2012;68:202-208
3. Eisenhardt SU, Habersberger J, Murphy A, Chen YC, Woollard KJ, Bassler N, Qian H, von Zur Muhlen C, Hagemeyer CE, Ahrens I, Chin-Dusting J, Bobik A, Peter K. Dissociation of pentameric to monomeric c-reactive protein on activated platelets localizes inflammation to atherosclerotic plaques. *Circ Res*. 2009;105:128-137
4. Ying SC, Gewurz H, Kinoshita CM, Potempa LA, Siegel JN. Identification and partial characterization of multiple native and neoantigenic epitopes of human c-reactive protein by using monoclonal antibodies. *J Immunol*. 1989;143:221-228
5. Strang F, Scheichl A, Chen YC, Wang X, Htun NM, Bassler N, Eisenhardt SU, Habersberger J, Peter K. Amyloid plaques dissociate pentameric to monomeric c-

reactive protein: A novel pathomechanism driving cortical inflammation in alzheimer's disease? *Brain Pathol.* 2012;22:337-346

6. Thiele JR, Goerendt K, Stark GB, Eisenhardt SU. Real-time digital imaging of leukocyte-endothelial interaction in ischemia-reperfusion injury (iri) of the rat cremaster muscle. *J Vis Exp.* 2012:e3973

7. Baatz H, Steinbauer M, Harris AG, Krombach F. Kinetics of white blood cell staining by intravascular administration of rhodamine 6g. *Int J Microcirc Clin Exp.* 1995;15:85-91

8. Lee HB, Blaufox MD. Blood volume in the rat. *J Nucl Med.* 1985;26:72-76

9. Maroko PR, Carpenter CB, Chiariello M, Fishbein MC, Radvany P, Knostman JD, Hale SL. Reduction by cobra venom factor of myocardial necrosis after coronary artery occlusion. *J Clin Invest.* 1978;61:661-670

10. Dumont EA, Reutelingsperger CP, Smits JF, Daemen MJ, Doevendans PA, Wellens HJ, Hofstra L. Real-time imaging of apoptotic cell-membrane changes at the single-cell level in the beating murine heart. *Nat Med.* 2001;7:1352-1355

11. Kuzkaya N, Weissmann N, Harrison DG, Dikalov S. Interactions of peroxynitrite with uric acid in the presence of ascorbate and thiols: Implications for uncoupling endothelial nitric oxide synthase. *Biochem Pharmacol.* 2005;70:343-354

12. Dikalov SI, Li W, Mehranpour P, Wang SS, Zafari AM. Production of extracellular superoxide by human lymphoblast cell lines: Comparison of electron spin resonance techniques and cytochrome c reduction assay. *Biochem Pharmacol.* 2007;73:972-980

13. Eisenhardt SU, Starke J, Thiele JR, Murphy A, Stark BG, Bassler N, Sviridov D, Winkler K, Peter K. Pentameric crp attenuates inflammatory effects of mmlDl by inhibiting mmlDl--monocyte interactions. *Atherosclerosis*. 2012;224:384-393